# Asymptotic safety in the Litim-Sannino model at four loops

A. V. Bednyakov[*] and A. I. Mukhaeva[†]
*Joint Institute for Nuclear Research, Joliot-Curie, 6, Dubna 141980, Russia*

(Received 19 January 2024; accepted 22 February 2024; published 29 March 2024)

We consider a four-dimensional $SU(N_c)$ gauge theory coupled to $N_f$ species of color fermions and $N_f^2$ colorless scalars. The quantum field theory possesses a weakly interacting ultraviolet fixed point that we determine from beta functions computed up to four-loop order in the gauge coupling, and up to three-loop order in the Yukawa and quartic scalar couplings. The fixed point has one relevant direction giving rise to asymptotic safety. We compute fixed-point values of dimensionless couplings together with the corresponding scaling exponents up to the first three nontrivial orders in Veneziano parameter $\epsilon$, both for infinite and finite number of colors $N_c$. We also consider anomalous dimensions for fields, scalar mass squared, and a class of dimension-three operators. Contrary to previous studies, we take into account possible mixing of the latter and compute eigenvalues of the corresponding matrix. Further, we investigate the size of the conformal window in the Veneziano limit and its dependence on $N_c$.

DOI: 10.1103/PhysRevD.109.065030

## I. INTRODUCTION

The study of asymptotic behavior of the dimensionless couplings in quantum field theory (QFT) provides important information both for the Standard Model (SM) and beyond the Standard Model (BSM) scenarios. One of these behaviors is known as asymptotic freedom [1,2], which is a defining feature of quantum chromodynamics. This behavior entails a decrease in the value of a coupling with the energy scale. Thus, in the deep ultraviolet (UV), this coupling tends to approach the Gaussian noninteractive fixed point (FP).

Asymptotic safety (AS) is an extension of the concept of asymptotic freedom, as outlined in the work of Weinberg [3]. In AS, the coupling in the deep UV also reaches a fixed point, but unlike in asymptotic freedom, the fixed-point value is not zero, which means that the theory remains interactive. Such theories are referred to as asymptotically safe.

The concept of asymptotic safety was initially introduced by S. Weinberg in the late 1970s as a means of achieving nonperturbative renormalizability for the four-dimensional theory of gravity [3]. However, in recent years, AS has been widely applied in the context of gauge theories to address issues with $U(1)$ gauge couplings (Landau pole) by stabilizing them at an interactive fixed point at a certain scale. Indications of AS has been found in simple [4,5], semisimple [6], and supersymmetric gauge theories coupled to matter [7–9]. From the phenomenological point of view, properties of such UV interactive fixed points for matter fields can be transmitted down to the low-energy regime and lead us to some phenomenological predictions; see, e.g., recent reviews [10,11].

An example of a UV-complete particle theory with a weakly interacting fixed point is a model of $N_f$ fermions coupled to $SU(N_c)$ gauge fields and elementary scalars through gauge and Yukawa interactions [5,12]. In the large-$N$ Veneziano limit, the fixed point can be systematically studied in perturbation theory using a small control parameter $\epsilon$, allowing for the extraction of specific details of theory. Previous studies [5,13–15] have identified critical couplings and universal exponents up to second order in $\epsilon$, including finite $N$ corrections. Phenomenological applications of the model and its extensions can be found in Refs. [15–33]. It is also worth mentioning that the model was the first nonsupersymmetric theory investigated in the large global charge limit [34,35]. The holographic description of the model was considered in Ref. [36].

In this paper, we confirm the study [37] of the UV critical theory and provide the fixed-point couplings and conformal data up to third order in $\epsilon$ (both for infinite and finite-$N_c$ scenarios) by considering four-loop gauge, three-loop Yukawa, and quartic $\beta$ functions. We also determine three-loop anomalous dimensions for dimension-three operators and discuss peculiarities in their computations as compared to Ref. [37].

The paper is organized as follows. Section II provides the main information about the considered model and operators.

[*]bednya@jinr.ru
[†]mukhaeva@theor.jinr.ru

In Sec. III we give the details of computation of the renormalization-group (RG) functions. In Sec. IV we demonstrate our results for fixed points, anomalous dimensions, and scaling exponents for finite $N_c$. The bounds on the conformal window are given in Sec. V. We conclude in Sec. VI. The full expressions for beta functions and various anomalous dimensions can be found in Appendixes A 1–A 3. Appendix B contains additional information related to finite-$N_c$ results.

## II. MODEL DESCRIPTION

We consider four-dimensional theory with $SU(N_c)$ gauge fields coupled to $N_f$ massless Dirac fermions and a scalar singlet field $H$. The last is uncharged under the gauge group and carries two flavor indices, such that it can be written as a $N_f \times N_f$ complex matrix. The corresponding Lagrangian is

$$\begin{aligned}\mathcal{L} = &-\frac{1}{4}F^{a\mu\nu}F^a_{\mu\nu} + \mathcal{L}_{gf} + \mathcal{L}_{gh} \\ &+ \mathrm{Tr}(\bar\psi i\hat D\psi) + \mathrm{Tr}(\partial^\mu H^\dagger \partial_\mu H) - y\mathrm{Tr}[\bar\psi(H\mathcal{P}_R + H^\dagger\mathcal{P}_L)\psi] \\ &- m^2\mathrm{Tr}(H^\dagger H) - u\mathrm{Tr}((H^\dagger H)^2) - v(\mathrm{Tr}(H^\dagger H))^2, \end{aligned} \tag{1}$$

where $F^a_{\mu\nu}$ is the field strength of the gauge bosons $G^a_\mu$ with $a = 1, \ldots, N_c^2 - 1$. The trace in Eq. (1) runs over both color and flavor indices and $\psi = \psi_L + \psi_R$ are fermions with $\mathcal{P}_{L/R} = \frac{1}{2}(1 \pm \gamma_5)$. In what follows, we use a linear $R_\xi$ gauge with $\mathcal{L}_{gf} = -\frac{1}{2\xi}(\partial_\mu G^a_\mu)^2$ together with the corresponding ghost Lagrangian $\mathcal{L}_{gh}$.

The theory (1) is invariant under global $G = U_L(N_f) \times U_R(N_f)$ "flavor" symmetry corresponding to independent unitary rotations of left- and right-handed chiral fermions. The matrix scalar field $H$ is colorless but transform under $G$ (see Table I). In this paper we also consider a class of operators that breaks the flavor symmetry down to diagonal $U(N_f)$. One can introduce independent couplings for these operators resulting in the following additional contribution to the Lagrangian (1):

$$\begin{aligned}\delta\mathcal{L} &= -m_\psi \mathrm{Tr}(\bar\psi\psi) - \frac{h_2}{2}[\mathrm{Tr}(HH^\dagger H) + \mathrm{H.c.}] \\ &\quad - \frac{h_3}{2}[\mathrm{Tr}(HH^\dagger)\mathrm{Tr}(H) + \mathrm{H.c.}] \\ &\equiv -m_\psi O_1 - h_2 O_2 - h_3 O_3 = -\vec\kappa\cdot\vec O. \end{aligned} \tag{2}$$

TABLE I. Representations of matter fields under gauge $SU(N_c)$ and flavor $U_L(N_f)$ and $U_R(N_f)$ groups.

| Field | $SU(N_c)$ | $U_L(N_f)$ | $U_R(N_f)$ |
|---|---|---|---|
| $\psi_L$ | $N_c$ | $N_f$ | 1 |
| $\psi_R$ | $N_c$ | 1 | $N_f$ |
| $H$ | 1 | $N_f$ | $\bar N_f$ |

The choice of the $G$-breaking terms is dictated by the fact that the operator $O_1 = \bar\psi\psi$, also considered in Ref. [37], mixes under renormalization with the two operators coupled to $h_{2,3}$.

The model has four dimensionless couplings: gauge coupling $g$, the Yukawa $y$, and two quartic scalar couplings $u$ and $v$. One usually introduces a set of rescaled couplings [38]

$$\begin{aligned}\alpha_g &= \frac{g^2 N_c}{(4\pi^2)}, \qquad \alpha_y = \frac{y^2 N_c}{(4\pi^2)}, \\ \alpha_u &= \frac{u N_f}{(4\pi^2)}, \qquad \alpha_v = \frac{v N_f^2}{(4\pi^2)}. \end{aligned} \tag{3}$$

The latter has been done since we consider the Veneziano limit [39] with $N_f, N_c \to \infty$. One also introduces a parameter

$$\epsilon \equiv \frac{N_f}{N_c} - \frac{11}{2} \tag{4}$$

that becomes continuous and may take any value between $(-\frac{11}{2}, \infty)$. The benefit of the Veneziano limit is that it allows systematic expansions in a small parameter. In our work we suppose that

$$0 < \epsilon \le 1, \tag{5}$$

and treat it as a small control parameter for perturbativity.

In order to study dimension-three operators in the Veneziano limit, we rescale the corresponding couplings and the operators as

$$m'_\psi = m_\psi\sqrt{N_c}, \qquad h'_2 = h_2 N_f, \qquad h'_3 = h_3 N_f^2, \tag{6}$$

$$O'_1 = O_1/\sqrt{N_c}, \quad O'_2 = O_2/N_f, \quad O'_3 = O_3/N_f^2. \tag{7}$$

This allows one to absorb all corrections with positive powers of $N_c$ and $N_f$ appearing in the beta functions for $\vec\kappa$ into the rescaled couplings given in Eqs. (3) and (6). It is worth noticing that the parameters $m_\phi$, $h_1$, and $h_2$ are rescaled in the same way as the dimensionless couplings $y$, $u$, and $v$, respectively.

## III. CALCULATION METHODS

The beta functions and anomalous dimensions in the $\overline{\mathrm{MS}}$ scheme can be computed by standard methods, so we omit full description of the techniques refereeing to appropriate literature. In this section, we only discuss peculiarities of the current calculation. Let us mention here that we do not rescale the couplings and operators according to Eqs. (3) and (6) in our explicit computation. The transition to the Veneziano-limit normalization is carried out at the final

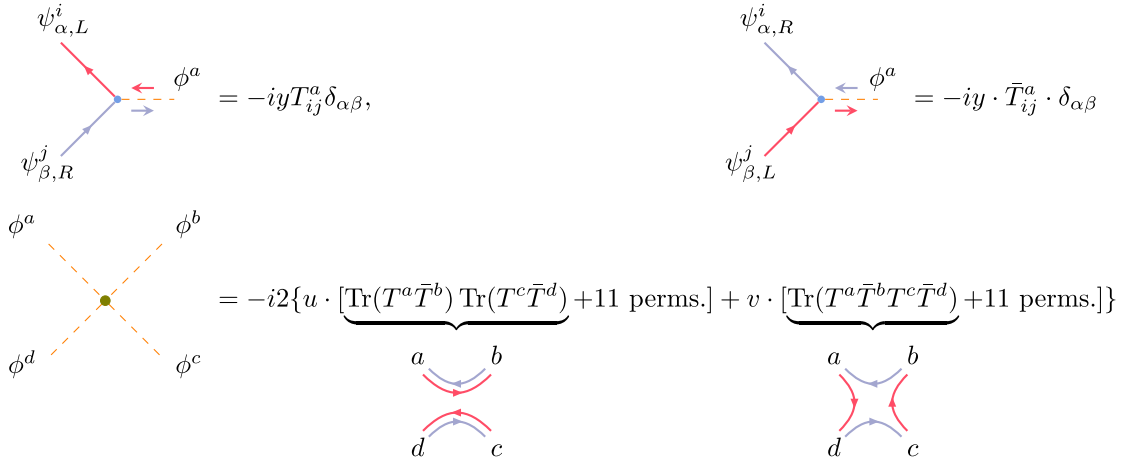


FIG. 1. Feynman rules for Yukawa and quartic vertices. The indices $i, j = 1, \ldots, N_f$ count fermion generations (flavor), while $\alpha, \beta = 1, \ldots, N_c$ correspond to the $SU(N_c)$ gauge group. Flavor flows for left- and right-handed fermions are indicated.

stage. Nevertheless, we present all our results in terms of $\alpha_{g,y,u,v}$ and for the rescaled operators (7).

In order to compute the required RG functions, we rewrite the Lagrangian (1) in terms of real scalars $\phi^a$ utilizing a decomposition ($a = 1, \ldots, 2N_f^2$) [40]

$$H = \phi^a T^a, \qquad H^\dagger = \phi^a \bar{T}^a, \qquad \bar{T}^a \equiv T^{a\dagger} \tag{8}$$

with $T^a$ being complex $N_f \times N_f$ matrices[1] normalized as

$$\mathrm{Tr}(T^a\bar{T}^b) + \mathrm{Tr}(T^b\bar{T}^a) = \delta^{ab} \tag{9}$$

and satisfying the following identities:

$$T^a_{ij}T^a_{kl} = \bar{T}^a_{ij}\bar{T}^a_{kl} = 0, \qquad T^a_{ij}\bar{T}^a_{kl} = \delta_{il}\delta_{jk}. \tag{10}$$

Such a decomposition gives rise to the Feynman rules (see Fig. 1) for the vertices involving $\phi^a$. In Fig. 1 we also indicate the flavor "flow" for the double-trace and single-trace scalar couplings that can be associated with the left ($L$) and right ($R$) chiral fermions. In the absence of $U_L(N_f) \times U_R(N_f)$ breaking, the "left-" and "right-handed" flows are "conserved" separately.

We implemented the rules in the DIANA [41] package based on QGRAF [42] and utilize FORM [43] to deal with index contractions and to compute Feynman integrals via the MATAD [44] code. In order to derive RG equations for $u$, $v$, and $y$, we generate Green's functions corresponding to radiative corrections for the tree-level Yukawa and quartic vertices up to three loops and extract local divergent terms by applying suitable projectors. Our explicit calculations heavily rely on well-known infrared rearrangement (IRR) trick [45,46], which allows one to deal only with fully massive vacuum integrals. The fermion-fermion-scalar interaction involves the $\gamma_5$ matrix, which requires special treatment in dimensional regularization (see, e.g., Ref. [47]). In this paper, we restrict ourselves to the seminaive approach [48,49] and by explicit computation we prove that potential ambiguities do not appear in the final result for the RG functions, thus, providing an independent cross-check of the results obtained in Ref. [37]. As for the four-loop gauge-coupling beta function the $\gamma_5$ ambiguity can be fixed by means of Weyl consistency conditions [50–53]. Moreover, we do not carry out explicit computations here, but use the RGBeta code [54] extended to 432 order in Refs. [55,56].

Let us now switch to the discussion of a family of dimension-three operators that includes $O_1 = \bar{\psi}\psi$. In dimensionally regularized theory[2] ($d = 4 - 2\varepsilon$) within the $\overline{\mathrm{MS}}$ scheme, we have a relation between bare and renormalized quantities

$$\begin{aligned}\vec{\kappa}_R \cdot [\vec{O}]_R &= \mu^{2\varepsilon} \cdot (\vec{\kappa})_0 \cdot (\vec{O})_0 \\ &= \mu^{2\varepsilon} \cdot (\vec{\kappa})_R \cdot \mathcal{Z}^T_\kappa \cdot \mathcal{Z}^{-1}_O \cdot [\vec{O}]_R,\end{aligned} \tag{11}$$

where all couplings in $\vec{\kappa}_R$, and all operators in $\vec{O}_R$ have in our case the mass dimension one and three, respectively. The corresponding renormalization matrices $\mathcal{Z}_\kappa$ and $\mathcal{Z}_O$ are defined as

$$\begin{aligned}\vec{\kappa}_0 &= \mathcal{Z}_\kappa(\mu, \alpha(\mu), \varepsilon) \cdot \vec{\kappa}_R, \\ \mathcal{Z}_\kappa(\mu, \alpha(\mu), \varepsilon) &= \begin{pmatrix} 1 & & \\ & \mu^\varepsilon & \\ & & \mu^\varepsilon \end{pmatrix} \cdot Z_\kappa(\alpha(\mu), \varepsilon),\end{aligned} \tag{12}$$

[1]One can also use a decomposition in terms of the identity matrix and $SU(N_f)$ generators as, e.g., in Refs. [34,35].

[2]Note the difference between the Veneziano parameter $\epsilon$ and that of dimensional regularization $\varepsilon$.

$$[\vec{O}]_R = \mathcal{Z}_O(\mu,\alpha(\mu),\varepsilon)\cdot(\vec{O})_0,$$
$$\mathcal{Z}_O(\mu,\alpha(\mu),\varepsilon) = Z_O(\alpha(\mu),\varepsilon)\cdot\begin{pmatrix}\mu^{2\varepsilon} & & \\ & \mu^{3\varepsilon} & \\ & & \mu^{3\varepsilon}\end{pmatrix}. \quad (13)$$

The renormalization matrices involve poles in $\varepsilon$ and depend on the renormalization scale $\mu$ together with the running dimensionless couplings from (1) denoted collectively by $\alpha(\mu)$. They satisfy

$$\mu^{2\varepsilon}\mathcal{Z}_\kappa^T = \mathcal{Z}_O \Rightarrow Z_\kappa^T = Z_O. \quad (14)$$

In what follows, we will routinely use $\mathcal{Z}$ and $Z$ to denote renormalization constants with and without explicit dependence on the renormalization scale $\mu$. The diagonal matrices involving powers of $\mu^\varepsilon$ account for mass dimensions of bare couplings and operators. We include them in the definition of $\mathcal{Z}$s for convenience, since we can write the beta functions of $\vec{\kappa}_R$ in a compact form

$$\frac{d}{d\ln\mu}\vec{\kappa} \equiv \dot{\vec{\kappa}} = \vec{\beta}_\kappa = \gamma_\kappa(\alpha)\cdot\vec{\kappa}$$
$$\gamma_\kappa(\alpha) = \dot{\mathcal{Z}}_\kappa^{-1}\cdot\mathcal{Z}_\kappa = -\mathcal{Z}_\kappa^{-1}\cdot\dot{\mathcal{Z}}_\kappa, \quad (15)$$

and relate the matrix anomalous dimension $\gamma_\kappa$ to the anomalous dimensions of the dimension-three operators

$$\gamma_O(\alpha) \equiv -\dot{\mathcal{Z}}_O\cdot\mathcal{Z}_O^{-1} = -2\varepsilon - \dot{\mathcal{Z}}_\kappa^T\cdot(\mathcal{Z}^T)_\kappa^{-1}$$
$$= -2\varepsilon + \gamma_\kappa^T(\alpha). \quad (16)$$

Both $\gamma_O(\alpha)$ and $\gamma_\kappa(\alpha)$ should be finite in the limit $\varepsilon\to 0$, which serves as a welcome check of the computation. As a consequence, in $d=4$ we have

$$\gamma_O = \gamma_\kappa^T. \quad (17)$$

This relation can be used in two ways. Given the beta functions of (a closed set of) the dimension-one couplings, one can extract the matrix anomalous dimension for the corresponding operators. In case we know $\gamma_O$, it is possible to reconstruct the $\overline{\text{MS}}$ beta functions for the operator couplings, e.g., via

$$\beta_{m_\psi} = m_\psi(\gamma_O)_{11} + h_2(\gamma_O)_{21} + h_3(\gamma_O)_{31}, \quad (18)$$

$$\beta_{h_2} = m_\psi(\gamma_O)_{12} + h_2(\gamma_O)_{22} + h_3(\gamma_O)_{32}, \quad (19)$$

$$\beta_{h_3} = m_\psi(\gamma_O)_{13} + h_2(\gamma_O)_{23} + h_3(\gamma_O)_{33}. \quad (20)$$

In this paper we explicitly carry out the renormalization of dimension-three operators and compute $\gamma_O$ up to three loops. In addition, we also cross-check our results at lower loops by adding (2) to the Litim-Sannino model (1) implemented in public computer codes ARGES [57] and RGBeta[3] [54] and computing $\vec{\beta}_\kappa$.

To find three-loop corrections to $Z_O$, we consider insertions of the operators $O_{1-3}$ into one-particle irreducible (1PI) Green's functions. The corresponding Feynman rules are given in Fig. 2. The renormalized 1PI Green's functions are finite and are related to the bare ones via

$$\langle[O^i]_R\cdot\tilde{O}^j\rangle_{1\text{PI}} = (Z_O)_{ik}\cdot\langle O_0^k\cdot\tilde{O}_0^j\rangle_{1\text{PI}}\cdot Z_{j,\text{ext}}. \quad (21)$$

Here $\tilde{O}_j$ is a product of external fields at different space-time points (either bare or renormalized) corresponding to the local operator $O_j$ with a property that $\langle O^i\cdot\tilde{O}^j\rangle_{\text{tree}}\propto\delta^{ij}$. The factors $Z_{j,\text{ext}}$ account for the external fields renormalization entering $\tilde{O}_j$, e.g., $Z_{1,\text{ext}} = Z_\psi$, $Z_{2,\text{ext}} = Z_{3,\text{ext}} = Z_H^{3/2}$ for $\psi_0 = \sqrt{Z_\psi}\cdot\psi$, and $H_0 = \sqrt{Z_H}\cdot H$. We determine the matrix elements of $(Z_O)_{ij}$ in the $\overline{\text{MS}}$ scheme order-by-order from the requirement that there are no $\varepsilon$ poles in the rhs (21).

It is important to stress that if we ignore $O_{2,3}$ [or the $h_{2,3}$ couplings in the Lagrangian (2)], we can compute $(Z_O)_{11}$ and $(\gamma_O)_{11}$ (the latter is denoted by $\gamma_{m_\psi}$ in Ref. [37]) by considering $\langle O_1(x)\psi(y)\bar{\psi}(z)\rangle_{1\text{PI}}$ up to the two-loop order without hitting any difficulties. At three loops there are diagrams [see, e.g., Fig. 3(a)], which require an insertion of the $O_2$ operator as a counterterm [Fig. 3(b)]. Because of this, we are forced to include $O_2$ in the game. The latter mixes with $O_1$ already at the one-loop order.[4] Moreover, starting from one loop, the $O_3$ operator is needed to account for all the divergences appearing in four-point functions $\langle O_2\phi^a\phi^b\phi^c\rangle_{1\text{PI}}$.

We also compute the divergences of the two-point functions $\langle O_i(x)\phi^a(y)\rangle_{1\text{PI}}$ for $i=1,2,3$ and extract the mixing of $O_i$ with $O_4 = 1/2(\partial^2\text{Tr}(H) + \text{H.c.})$, thus, modifying (13) as

$$[\vec{O}]_R = \mathcal{Z}_O\cdot(\vec{O})_0 + \vec{\mathcal{Z}}(O_4)_0, \quad (22)$$

$$[O_4]_R = \mathcal{Z}_H^{-1/2}(O_4)_0 \quad (23)$$

This gives rise to a $4\times 4$ mixing renormalization matrix $\bar{\mathcal{Z}}$ entering

$$[O_i]_R = (\bar{\mathcal{Z}}_O)_{ij}(O_j)_0, \qquad \bar{\mathcal{Z}}_O = \bar{Z}_O\cdot\begin{pmatrix}\mu^{2\epsilon} & & & \\ & \mu^{3\epsilon} & & \\ & & \mu^{3\epsilon} & \\ & & & \mu^{\epsilon}\end{pmatrix},$$
$$\bar{\gamma}_O = -\dot{\bar{Z}}_O\cdot\bar{Z}_O^{-1} \quad (24)$$

[3]Correct treatment of dimension-one couplings is implemented in RGBeta since version 1.1.5.

[4]Speaking in other terms, the sole introduction of $m_\psi$ in (2) will radiatively generate a $h_2$ coupling at one-loop level [corresponding to a grey blob in Fig. 3(a)].

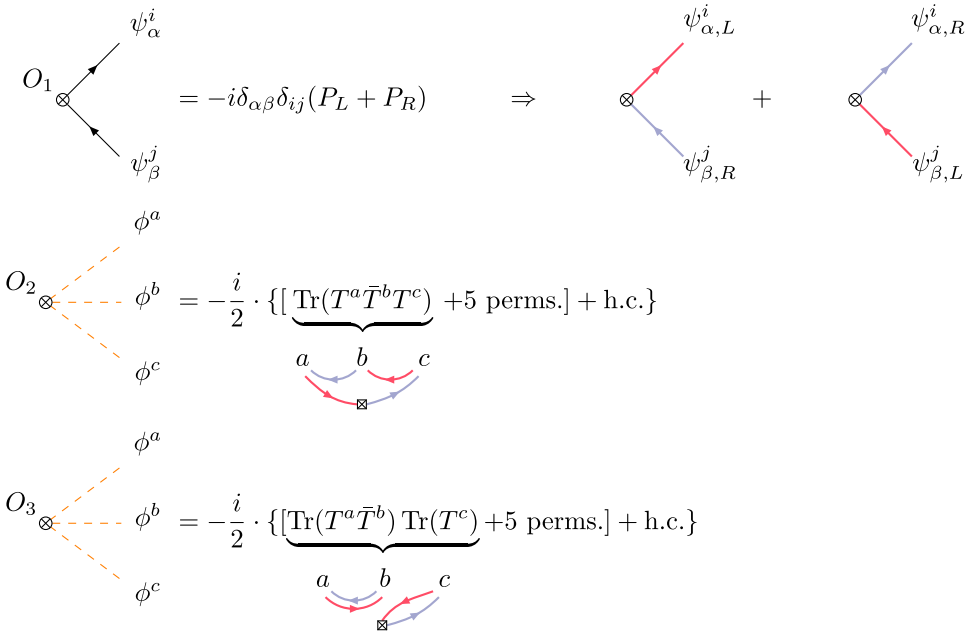


FIG. 2. Feynman rules for dimension-three operators. All the operators break the flavor symmetry $G$ by "flipping" the "chirality" of the flavor flow, which in the case of scalar operators we indicate by a box with a cross inside.

where $i = 1, \ldots, 4$ and $\bar{Z}_O$ is schematically depicted in Fig. 4. If we take into account the equations of motion (EOM) for the bare operators

$$\begin{aligned}(O_4)_0 + \vec{\Lambda}_0 \cdot (\vec{O})_0 &= 0,\\ \vec{\Lambda}_0 &= \{y_0/2, 2u_0, 2v_0\}\\ &\equiv \{\mu^\varepsilon Z_y(y/2), \mu^{2\varepsilon} Z_u(2u), \mu^{2\varepsilon} Z_v(2v)\}\end{aligned} \tag{25}$$

where $Z_{y,u,v}$ are renormalization constants for the corresponding couplings, and express $O_4$ as a linear combination of $\vec{O}$, we obtain another $3 \times 3$ matrix

$$\mathcal{Z}_O \to \tilde{\mathcal{Z}}_O \equiv \mathcal{Z}_O - \vec{\mathcal{Z}} \otimes \vec{\Lambda}_0, \tag{26}$$

schematically presented in Fig. 5. The corresponding anomalous dimension is given by

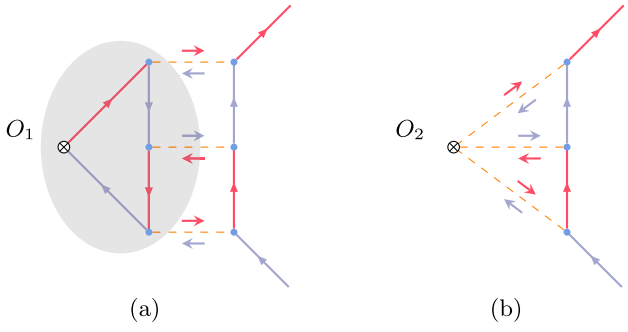


FIG. 3. A three-loop diagram (a) with a $O_1 = \bar{\psi}\psi$ insertion that requires a two-loop counterterm due to $O_2$ (b). The grey blob gives rise to a one-loop contribution to $(Z_O)_{21}$.

$$\tilde{\gamma}_O \equiv -\dot{\tilde{\mathcal{Z}}}_O \cdot \tilde{\mathcal{Z}}_O^{-1} \tag{27}$$

and is different from $\gamma_O$ (16). At a fixed point, $\tilde{\gamma}^*_O$ ($\gamma^*_O$) has a eigenvalue $\gamma^*_H$ ($-\gamma^*_H$). The other two eigenvalues of $\gamma^*_O$ coincide with those of $\tilde{\gamma}^*_O$. This can be interpreted as the fact that only two of the considered dimension-three eigenoperators are independent, while the remaining one is a descendent of $\mathrm{Tr}(H) + \mathrm{H.c.}$

Before discussing results, let us note how our approach differs from that of Ref. [37]. The authors of Ref. [37] utilized the same IRR technique and the seminaive treatment of $\gamma_5$ in their three-loop calculations. However, instead of DIANA and MATAD, they used a private framework to deal with Feynman diagrams generated by QGRAF. In our study we *do not* rely on the dummy-field method (see, e.g., Ref. [58] and references therein) to derive the beta functions of dimensional couplings, but extract them from Green's functions with insertions of the corresponding operators. Moreover, the authors of Ref. [37] considered only the $O_1 = \bar{\psi}\psi$ operator and did not account for possible mixing with $O_{2,3}$. Because of this, the anomalous dimension[5] denoted by $\gamma_{m_\psi}$ is *not* an eigenvalue of the corresponding matrix and, if computed at a fixed point, does *not* represent a correction to canonical scaling.

In what follows, we present all our results in terms of rescaled couplings and for the rescaled operators $O'$ (7). All expressions are available in computer-readable form as Supplemental Material [59].

[5]Corresponding to $(\gamma_O)_{11} = (\gamma_\kappa)_{11}$ in our notation.

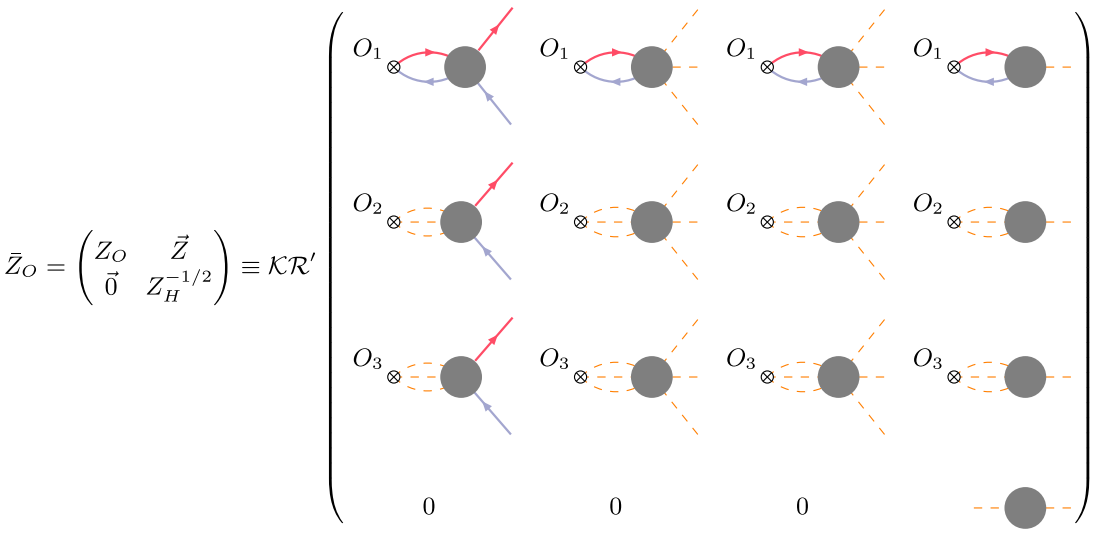


FIG. 4. One-particle-irreducible Green's functions used to extract matrix elements of $Z_O$. The factor $Z_H^{-1/2}$ enters the matrix $\bar{Z}_O$ due to $[O_4]_R = Z_H^{-1/2}(O_4)_0$.

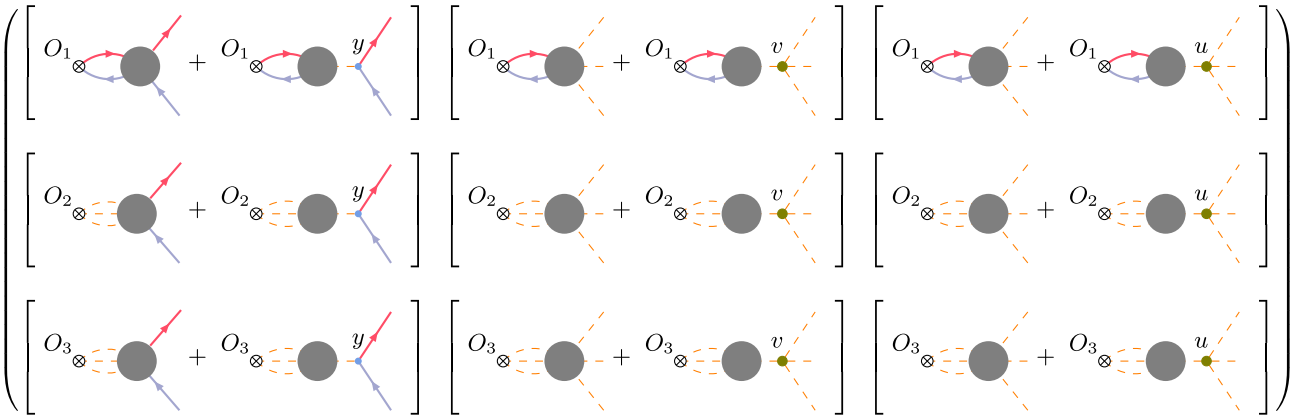


FIG. 5. Green's functions used to extract anomalous dimensions $\tilde{\gamma}_O$ of the dimensions-three operators with the account of equations of motion, expressing $O_4$ as a linear combination of $O_{1-3}$.

## IV. RESULTS

In this section, we summarize our results for $\beta$ functions for (in)finite $N_c$ and anomalous dimensions. Moreover, we determine fixed points and universal scaling dimensions up to the third nontrivial order in the Veneziano parameter also for both cases.

### A. Fixed points

As it is well known in perturbation theory the $\beta$ functions can be given as

$$\beta_x \equiv \frac{d\alpha_x}{d\ln\mu} = \beta_x^{(1)} + \beta_x^{(2)} + \beta_x^{(3)} + \cdots, \tag{28}$$

where $\beta_x^{(n)}$ denotes the $n$th loop contribution, and $x = \{g, y, u, v\}$. In Ref. [37] they were found for the first time and provided both in the Veneziano limit and with finite-$N_c$ corrections. We recomputed them independently and provide the lengthy expressions in Appendix A 1 and as Supplemental Material [59].

Using the 433-order $\beta$ functions and solving $\beta_i(\alpha_j^*) = 0$ systematically, we determine interacting fixed points up to complete third order in the small parameter $\epsilon$. We expressed fixed points as a series expansion

$$\alpha_x^* = c_x^{(1)} f_x^{(1)}(N_c)\epsilon + c_x^{(2)} f_x^{(2)}(N_c)\epsilon^2 + c_x^{(3)} f_x^{(3)}(N_c)\epsilon^3 + O(\epsilon^4), \tag{29}$$

where $x = \{g, y, u, v\}$. We have six possible solutions with fixed points; however, following Refs. [5,6,14], we choose a fully interacting UV fixed point ($\alpha_{g,y,u,v}^* \neq 0$) that exhibits asymptotically safe behavior.

The coefficients $c_x^{(i)}$ of series expansion can be found by solving the beta functions in this limit order by order for the stationary point. We recomputed the exact expressions for $c_x^{(i)}$ and found agreement with Ref. [37]

$$c_g^{(1)} = \frac{26}{57}, \qquad c_g^{(2)} = -\frac{23(13068\sqrt{23} - 75245)}{370386}, \tag{30}$$

$$c_g^{(3)} = \frac{(5025189312\zeta_3 + 353747709269 - 71703657432\sqrt{23})}{2406768228}, \tag{31}$$

$$c_y^{(1)} = \frac{4}{19}, \qquad c_y^{(2)} = \frac{(43549 - 6900\sqrt{23})}{20577}, \tag{32}$$

$$c_y^{(3)} = \frac{(29734848\zeta_3 + 2893213181 - 580847448\sqrt{23})}{44569782}, \tag{33}$$

$$c_u^{(1)} = \frac{\sqrt{23} - 1}{19}, \qquad c_u^{(2)} = \frac{365825\sqrt{23} - 1476577}{631028}, \tag{34}$$

$$c_u^{(3)} = \left(\frac{5173524931447\sqrt{23} - 24197965967251}{282928976136} - \frac{416(\sqrt{23} - 12)\zeta_3}{6859}\right), \tag{35}$$

$$c_v^{(1)} = \frac{\sqrt{2(10 + 3\sqrt{23})} - 2\sqrt{23}}{19}, \tag{36}$$

$$c_v^{(2)} = \frac{268229312 - 68836310\sqrt{23} + 46652027\sqrt{2(10 + 3\sqrt{23})} - 9153184\sqrt{46(10 + 3\sqrt{23})}}{67519996}, \tag{37}$$

$$\begin{aligned} c_v^{(3)} = +\frac{1}{3239253847781064}[&498710025259776\zeta_3 - 105786975055104\sqrt{23}\zeta_3 \\ &+6742118880147456\sqrt{2(10 + 3\sqrt{23})}\zeta_3 - 1374312631206528\sqrt{46(10 + 3\sqrt{23})}\zeta_3 \\ &+479791813615522776 - 103064713697904086\sqrt{23} + 74641138195038841\sqrt{2(10 + 3\sqrt{23})} \\ &-15585870376520334\sqrt{46(10 + 3\sqrt{23})}]. \end{aligned} \tag{38}$$

For convenience, we provide the numerical results in the Veneziano limit [37]

$$\alpha_g^* = 0.456\epsilon + 0.781\epsilon^2 + 6.610\epsilon^3 + \mathbf{24.137}\epsilon^4, \tag{39}$$

$$\alpha_y^* = 0.211\epsilon + 0.508\epsilon^2 + 3.322\epsilon^3 + \mathbf{15.212}\epsilon^4, \tag{40}$$

$$\alpha_u^* = 0.200\epsilon + 0.440\epsilon^2 + 2.693\epsilon^3 + \mathbf{12.119}\epsilon^4, \tag{41}$$

$$-\alpha_v^* = 0.137\epsilon + 0.632\epsilon^2 + 4.313\epsilon^3 + \mathbf{24.147}\epsilon^4, \tag{42}$$

where we also include subleading terms $\mathcal{O}(\epsilon^4)$ terms that will be modified when the 544-result will be available [37]. In addition, Table II shows various $\beta_x^{(l)}$ evaluated at the fixed point $(\alpha_g^*, \alpha_y^*, \alpha_u^*, \alpha_v^*)$ given above. One sees the typical size of the coefficients that cancel at each order of $\epsilon$ expansion up to $\mathcal{O}(\epsilon^5)$ in $\beta_g$, and up to $\mathcal{O}(\epsilon^4)$ in other beta functions. Subleading terms that do not add up to zero due to missing high-order corrections are also indicated.

The functions $f_x^{(i)}$ first introduced in Ref. [14] capture the dependence on $N_c$ and can be computed in the same

TABLE II. The model beta functions at the fixed point as series in $\epsilon$. Cancellations between contributions from different loop orders are presented up to $\mathcal{O}(\epsilon^5)$ for $\beta_g$ and up to $\mathcal{O}(\epsilon^4)$ for $\beta_{y,u,v}$. Higher-order terms marked by boldface are not reliably calculated and are not summed up to zero, but (the sum) can be used to estimate the size of typical high-order contribution.

| | $\epsilon^3$ | $\epsilon^4$ | $\epsilon^5$ | $\epsilon^6$ |
|---|---|---|---|---|
| $\beta_g^{(1)}$ | 0.277419 | 0.94969 | 8.85345 | **13.7629** |
| $\beta_g^{(2)}$ | −0.277419 | −3.42714 | −24.4312 | **−120.131** |
| $\beta_g^{(3)}$ | 0 | 2.47745 | 19.7319 | **209.597** |
| $\beta_g^{(4)}$ | 0 | 0 | −4.15417 | **−37.2974** |
| $\beta_g$ | 0 | 0 | 0 | **65.9311** |

| | $\epsilon^3$ | $\epsilon^4$ | $\epsilon^5$ |
|---|---|---|---|
| $\beta_y^{(1)}$ | 0.49336 | 1.8551 | **10.4922** |
| $\beta_y^{(2)}$ | −0.49336 | −3.11773 | **−28.4972** |
| $\beta_y^{(3)}$ | 0 | 1.26263 | **6.86205** |
| $\beta_y^{(4)}$ | 0 | 0 | ⋯ |
| $\beta_y$ | 0 | 0 | **−11.143** |

| | $\epsilon^3$ | $\epsilon^4$ | $\epsilon^5$ |
|---|---|---|---|
| $\beta_u^{(1)}$ | −0.258097 | −2.26905 | **−9.06296** |
| $\beta_u^{(2)}$ | 0.258097 | 2.52154 | **22.1462** |
| $\beta_u^{(3)}$ | 0 | −0.252485 | **−3.72929** |
| $\beta_u^{(4)}$ | 0 | 0 | ⋯ |
| $\beta_u$ | 0 | 0 | **9.3539** |

| | $\epsilon^3$ | $\epsilon^4$ | $\epsilon^5$ |
|---|---|---|---|
| $\beta_v^{(1)}$ | −0.992548 | −9.26177 | **−24.2444** |
| $\beta_v^{(2)}$ | 0.992548 | 9.04913 | **82.5704** |
| $\beta_v^{(3)}$ | 0 | 0.212636 | **−10.4633** |
| $\beta_v^{(4)}$ | 0 | 0 | ⋯ |
| $\beta_v$ | 0 | 0 | **47.8627** |

manner as the $c_x^{(i)}$. It should be noted that $\lim_{N_c\to\infty} f_x^{(i)} \equiv 1$, which means that the FPs found for in(finite) cases are connected continuously. Therefore, for the infinite-$N_c$ case we have only $c_x^{(i)}$, which are exact numbers. However, the full form of $f_x^{(i)}$ is complicated.[6] Because of this, following the ideas of [57], we fitted all the finite-$N_c$ corrections in the range $N_c \in [3, 100]$ as ratios of two second-order polynomials up to $\epsilon^3$. The results can be found in Appendix B. Then, we carried out another fit when ratios of two fourth-order polynomials were considered and obtained the following expressions:

$$f_g^{(1)} = \frac{N_c^2}{N_c^2 - \frac{110}{19}}, \qquad f_g^{(2)} = \frac{N_c^4 - 0.534N_c^2 + 2.485}{N_c^4 - 13.106N_c^2 + 43.594},$$
$$f_g^{(3)} = \frac{N_c^4 + 8.103N_c^2 + 40.270}{N_c^4 - 15.278N_c^2 + 59.731}, \tag{43}$$

$$f_y^{(1)} = \frac{N_c^2 - 1}{N_c^2 - \frac{110}{19}}, \qquad f_y^{(2)} = \frac{N_c^4 - 0.976N_c^2 + 1.185}{N_c^4 - 12.691N_c^2 + 40.681},$$
$$f_y^{(3)} = \frac{N_c^4 + 6.520N_c^2 + 32.220}{N_c^4 - 15.226N_c^2 + 59.311}, \tag{44}$$

$$f_u^{(1)} = \frac{N_c^4 - 1.047N_c^2 + 0.047}{N_c^4 - 5.863N_c^2 + 0.428},$$
$$f_u^{(2)} = \frac{N_c^4 - 1.049N_c^2 + 1.545}{N_c^4 - 12.779N_c^2 + 41.292},$$
$$f_u^{(3)} = \frac{N_c^4 + 7.239N_c^2 + 35.870}{N_c^4 - 15.284N_c^2 + 59.770}, \tag{45}$$

$$f_v^{(1)} = \frac{N_c^4 - 1.029N_c^2 + 0.029}{N_c^4 - 5.878N_c^2 + 0.511},$$
$$f_v^{(2)} = \frac{N_c^4 - 1.718N_c^2 + 1.0112}{N_c^4 - 12.330N_c^2 + 38.240},$$
$$f_v^{(3)} = \frac{N_c^4 + 4.258N_c^2 + 19.300}{N_c^4 - 14.946N_c^2 + 56.311}. \tag{46}$$

which turn out to be more accurate. The maximal value of the mean squared error (MSE) for the $f_x^{(i)}$ with our fourth (second) order polynomial fits in each order of $\epsilon$ is as follows: $10^{-12}$ $(4\times10^{-11})$, $10^{-9}$ $(8\times10^{-5})$, $8\times10^{-5}$ $(4\times10^{-3})$. While the fit with the second-order polynomials seems to provide good approximation, we restrict ourselves to a more precise fourth-order result.

At the end, we carry our numerical comparison of the two types of fits and exact results. The green dashed line in Fig. 6 corresponds to the second-order fit (see Appendix B), and purple solid line is our fourth-order fit (43)–(46). One can see that the green dashed line "misses" exact points in Fig. 6 in the presented range of $N_c$, while the purple line goes through the dots.

### B. Critical exponents

Let us study the universal critical exponents. The latter can be obtained as the eigenvalues of the stability matrix

$$M_{ij} = \left.\frac{\partial\beta_i}{\partial\alpha_j}\right|_{\alpha=\alpha^*}, \tag{47}$$

which again we expand as a power series

[6]Available by demand from the authors.

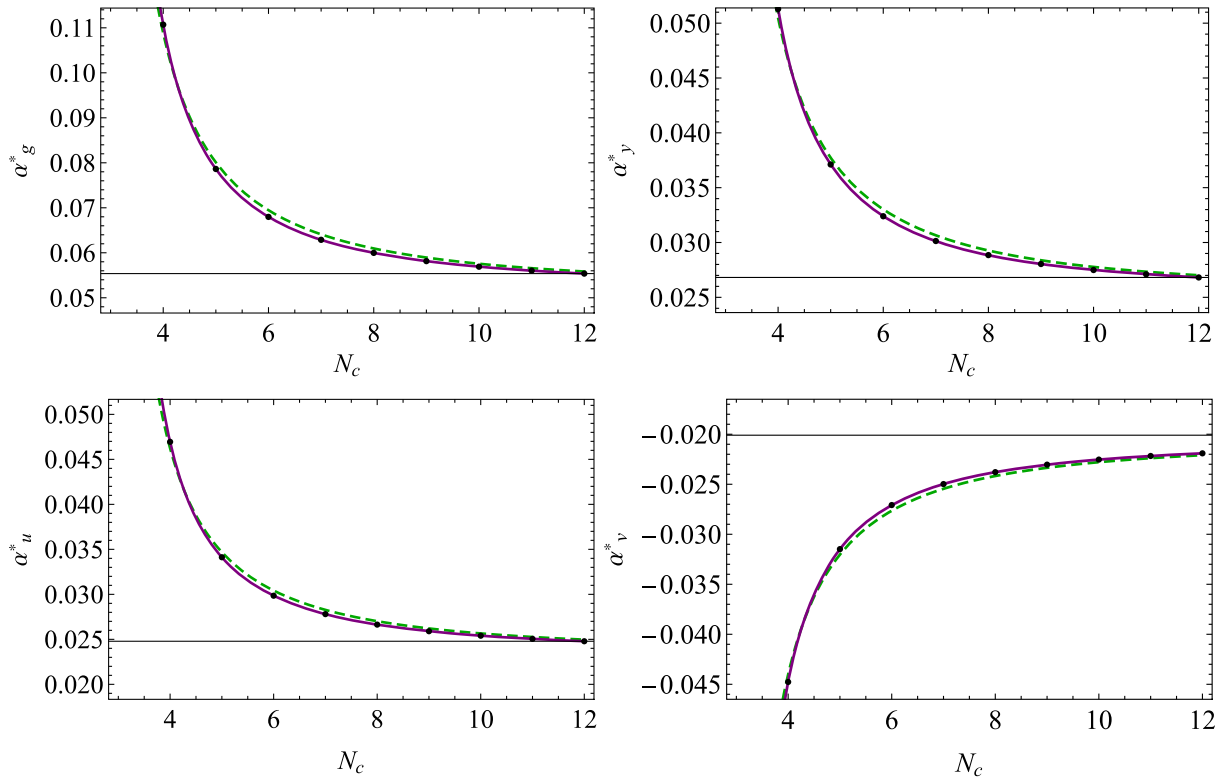


FIG. 6. The dependence of couplings from the number of colors $N_c$ for fixed $\epsilon = 0.09$. Here the purple line is our fourth-order polynomial fit (43)–(46), the green dashed line is second-order fit (B1). The black dots correspond to exact values. It should be noted that we omit the point $N_c = 3$, since it lies higher in the FP's scale, therefore the difference between the fits is not clearly visible.

$$\theta_j = c^{(1)}_{\theta_j} f^{(1)}_{\theta_j} \epsilon + c^{(2)}_{\theta_j} f^{(2)}_{\theta_j} \epsilon^2 + c^{(3)}_{\theta_j} f^{(3)}_{\theta_j} \epsilon^3 + \cdots \tag{48}$$

and find perfect agreement with [37] (note that for $\theta_1$ expansion starts at $\epsilon^2$ so $c^{(1)}_{\theta_1} = 0$):

$$c^{(2)}_{\theta_1} = -\frac{104}{171}, \qquad c^{(3)}_{\theta_1} = \frac{2296}{3249}, \qquad c^{(4)}_{\theta_1} = \frac{(43551640704\zeta_3 + 1405590649319 - 281341851912\sqrt{23})}{15643993482}, \tag{49}$$

$$c^{(1)}_{\theta_2} = \frac{52}{19}, \quad c^{(2)}_{\theta_2} = \frac{(136601719 - 22783308\sqrt{23})}{4094823}, \quad c^{(3)}_{\theta_2} = \frac{5(547695099865475491 - 111718308712462080\sqrt{23})}{2692813775855538}, \tag{50}$$

$$c^{(1)}_{\theta_3} = \frac{8}{19}\sqrt{20 + 6\sqrt{23}}, \qquad c^{(2)}_{\theta_3} = \frac{2(45155739 - 9153184\sqrt{23})\sqrt{20 + 6\sqrt{23}}}{16879999}, \tag{51}$$

$$c^{(3)}_{\theta_3} = \frac{\sqrt{20 + 6\sqrt{23}}(-918044509824(1497\sqrt{23} - 7558)\zeta_3 + 73205713038142585 - 15289473238519518\sqrt{23})}{404906730972633}, \tag{52}$$

$$c^{(1)}_{\theta_4} = \frac{16\sqrt{23}}{19}, \qquad c^{(2)}_{\theta_4} = \frac{4(68248487\sqrt{23} - 255832864)}{31393643}, \tag{53}$$

$$c^{(3)}_{\theta_4} = \frac{2(37418532792608300581\sqrt{23} - 174067504271892880236)}{278706225801048183}. \tag{54}$$

Numerical evaluation of these coefficients gives in the Veneziano limit [37]

$$-\theta_1 = 0.608\epsilon^2 - 0.707\epsilon^3 - 6.947\epsilon^4 - \mathbf{4.825}\epsilon^5, \quad (55)$$

$$\theta_2 = 2.737\epsilon + 6.676\epsilon^2 + 22.120\epsilon^3 + \mathbf{102.55}\epsilon^4, \quad (56)$$

$$\theta_3 = 2.941\epsilon + 1.041\epsilon^2 + 5.137\epsilon^3 - \mathbf{62.340}\epsilon^4, \quad (57)$$

$$\theta_4 = 4.039\epsilon + 9.107\epsilon^2 + 38.646\epsilon^3 + \mathbf{87.016}\epsilon^4 \quad (58)$$

and for not too large $\epsilon$ (see below) there is only one relevant direction corresponding to $\theta_1 < 0$ giving rise to an asymptotically safe scenario. In Eq. (58) we again highlight terms that are not determined precisely in the 433 approximation and will be modified by high-order terms.

Finite-$N_c$ corrections are incorporated in the factors, which we approximate as[7]:

$$f^{(2)}_{\theta_1} = \frac{N_c^2}{N_c^2 - \frac{110}{19}}, \qquad f^{(3)}_{\theta_1} = \frac{N_c^2\left(N_c^2 - \frac{326}{287}\right)}{\left(N_c^2 - \frac{110}{19}\right)^2},$$
$$f^{(4)}_{\theta_1} = \frac{N_c^4 + 10.21N_c^2 + 49.2}{N_c^4 - 15.23N_c^2 + 59.44}, \quad (59)$$

$$f^{(1)}_{\theta_2} = \frac{N_c^2 - 1}{N_c^2 - \frac{110}{19}}, \qquad f^{(2)}_{\theta_2} = \frac{N_c^4 - 0.8198N_c^2 + 0.33}{N_c^4 - 12.667N_c^2 + 40.51},$$
$$f^{(3)}_{\theta_2} = \frac{N_c^4 + 8.568N_c^2 + 44.8}{N_c^4 - 15.70N_c^2 + 63.07}, \quad (60)$$

$$f^{(1)}_{\theta_3} = \frac{N_c^4 - 0.3883N_c^2 - 0.6036}{N_c^4 - 5.265N_c^2 - 3.04},$$
$$f^{(2)}_{\theta_3} = \frac{N_c^4 - 1.580N_c^2 + 3.753}{N_c^4 - 12.767N_c^2 + 41.189},$$
$$f^{(3)}_{\theta_3} = \frac{N_c^4 + 11.09N_c^2 + 48.6}{N_c^4 - 15.42N_c^2 + 60.86}, \quad (61)$$

$$f^{(1)}_{\theta_4} = \frac{N_c^4 - 0.7726N_c^2 - 0.2459}{N_c^4 - 5.392N_c^2 - 2.30},$$
$$f^{(2)}_{\theta_4} = \frac{N_c^4 + 16.58N_c^2 - 11}{N_c^4 - 13.33N_c^2 + 45.33},$$
$$f^{(3)}_{\theta_4} = \frac{N_c^4 + 61.95N_c^2 + 357}{N_c^4 - 15.64N_c^2 + 62.73}. \quad (62)$$

The maximal value of MSE for the given (second-order result from the Appendix B) approximations are $10^{-19}$ ($10^{-10}$), $10^{-10}$ ($10^{-3}$), and $10^{-7}$ (0.15) for first, second, and third nontrivial orders in $\epsilon$.

### C. Other anomalous dimensions

In this subsection we provide results for the scalar and fermion anomalous dimensions. In addition, we consider the operator $\mathrm{Tr}(H^\dagger H)$ coupled to $m^2$ in (1) together with the anomalous dimensions corresponding to dimension-three eigenoperators discussed earlier. The full expressions for anomalous dimensions beyond the Veneziano limit can be found in Appendix A 3 and are also available in the Supplemental Material [59].

At the fixed point the anomalous dimensions are given as a series expansion in $\epsilon$. In the Veneziano limit we have gauge-independent coefficients

$$c_H^{(1)} = \frac{4}{19}, \qquad c_H^{(2)} = \frac{14567}{6859} - \frac{2376\sqrt{23}}{6859}, \qquad c_H^{(3)} = \frac{8816623159}{133709346} - \frac{753675598}{2476099\sqrt{23}}, \quad (63)$$

for the scalar fields, and

$$c_\psi^{(1)} = \frac{11}{19}, \quad c_\psi^{(2)} = \frac{3738501 - 683100\sqrt{23}}{740772}, \quad c_\psi^{(3)} = \frac{2879380764\zeta(3) + 780746553081 - 158608932408\sqrt{23}}{4813536456}, \quad (64)$$

which is valid in the Landau gauge $\xi = \xi^* = 0$ (see also Ref. [37]). The gauge-independent result for $m^2$ can be cast into

$$c_{m^2}^{(1)} = \frac{4}{19}\sqrt{2(10 + 3\sqrt{23})}, \quad c_{m^2}^{(2)} = \frac{(45155739 - 9153184\sqrt{23})\sqrt{20 + 6\sqrt{23}}}{16879999},$$
$$c_{m^2}^{(3)} = \frac{\sqrt{20 + 6\sqrt{23}}(-918044509824(1497\sqrt{23} - 7558)\zeta(3) + 73205713038142585 - 15289473238519518\sqrt{23})}{809813461945266}, \quad (65)$$

[7]It is interesting that our fourth-order fit for $f^{(3)}_{\theta_1}$ gives "exact result," which we were not able to reproduce analytically. Yet numerical comparison up to 10000 digits shows no difference.

while gluon ($G$) and ghost ($c$) field anomalous dimensions in the Landau gauge[8] are given as

$$c_G^{(1)} = -2c_c^{(1)} = \frac{13}{19}, \qquad c_G^{(2)} = -2c_c^{(2)} = \frac{188725 - 33396\sqrt{23}}{27436},$$
$$c_G^{(3)} = -2c_c^{(3)} = \frac{288694588\zeta(3) + 38849548925 - 7884584928\sqrt{23}}{178279128}. \tag{66}$$

Substituting the coefficients into the power series, we have in the Veneziano limit and (for $\xi = 0$) [37]

$$\gamma_H = 0.2105\epsilon + 0.4625\epsilon^2 + 2.4711\epsilon^3, \tag{67}$$

$$\gamma_\psi = 0.5789\epsilon + 0.6243\epsilon^2 + 4.8916\epsilon^3, \tag{68}$$

$$\gamma_{m^2} = 1.4703\epsilon + 0.5207\epsilon^2 + 2.5684\epsilon^3, \tag{69}$$

$$\gamma_G = -2\gamma_c = 0.6842\epsilon + 1.0411\epsilon^2 + 7.7599\epsilon^3. \tag{70}$$

The factors that account for the finite-$N_c$ corrections are again approximated as

$$f_H^{(1)} = \frac{N_c^2 - 1}{N_c^2 - \frac{110}{19}}, \qquad f_H^{(2)} = \frac{N_c^4 - 0.819N_c^2 + 1.265}{N_c^4 - 12.747N_c^2 + 41.073}, \qquad f_H^{(3)} = \frac{N_c^4 + 8.310N_c^2 + 41.460}{N_c^4 - 15.354N_c^2 + 60.340}, \tag{71}$$

$$f_\psi^{(1)} = \frac{N_c^2 - 1}{N_c^2 - \frac{110}{19}}, \qquad f_\psi^{(2)} = \frac{N_c^4 + 0.459N_c^2 + 3.821}{N_c^4 - 13.218N_c^2 + 44.414}, \qquad f_\psi^{(3)} = \frac{N_c^4 + 10.100N_c^2 + 51.904}{N_c^4 - 15.483N_c^2 + 61.368}, \tag{72}$$

$$f_{m^2}^{(1)} = \frac{N_c^4 - 2.678N_c^2 + 1.677}{N_c^4 - 7.468N_c^2 + 9.715}, \qquad f_{m^2}^{(2)} = \frac{N_c^4 + 9.603N_c^2 + 11.895}{N_c^4 - 13.542N_c^2 + 46.829}, \qquad f_{m^2}^{(3)} = \frac{N_c^4 + 47.739N_c^2 + 253.184}{N_c^4 - 15.868N_c^2 + 64.530}, \tag{73}$$

$$f_{G(c)}^{(1)} = \frac{N_c^2}{N_c^2 - \frac{110}{19}}, \qquad f_{G(c)}^{(2)} = \frac{N_c^4 - 0.522N_c^2 + 3.152}{N_c^4 - 13.217N_c^2 + 44.395}, \qquad f_{G(c)}^{(3)} = \frac{N_c^4 + 9.086N_c^2 + 48.136}{N_c^4 - 15.440N_c^2 + 61.028}, \tag{74}$$

where the maximal MSE is no worse than $3 \times 10^{-7}$ in comparison to $10^{-1}$ for the approximations given in Eq. (B2).

Finally, the eigenvalues for the dimension-three operator $4 \times 4$ anomalous dimension matrix are given by

$$\gamma_j = c_{\gamma_j}^{(1)} f_{\gamma_j}^{(1)} \epsilon + c_{\gamma_j}^{(2)} f_{\gamma_j}^{(2)} \epsilon^2 + c_{\gamma_j}^{(3)} f_{\gamma_j}^{(3)} \epsilon^3 + \cdots \tag{75}$$

with

$$c_{\gamma_1}^{(1)} = -c_{\gamma_2}^{(1)} = c_H^{(1)} \qquad c_{\gamma_1}^{(2)} = -c_{\gamma_2}^{(2)} = c_H^{(2)} \qquad c_{\gamma_1}^{(3)} = -c_{\gamma_2}^{(3)} = c_H^{(3)} \tag{76}$$

$$c_{\gamma_3}^{(1)} = \frac{4}{19}(1 + 2\sqrt{23}), \qquad c_{\gamma_3}^{(2)} = \frac{606162}{6859\sqrt{23}} - \frac{99745}{6859}, \qquad c_{\gamma_3}^{(3)} = \frac{4207372301377}{1537657479\sqrt{23}} - \frac{73545557081}{133709346}. \tag{77}$$

$$c_{\gamma_4}^{(1)} = \frac{4}{19}\left(1 + \sqrt{20 + 6\sqrt{23}}\right), \tag{78}$$

$$c_{\gamma_4}^{(2)} = \frac{14567}{6859} - \frac{2376\sqrt{23}}{6859} + \frac{\sqrt{2(1475668498887\sqrt{23} - 7061359720318)}}{6859\sqrt{2461}}, \tag{79}$$

[8]The result $\gamma_G = -2\gamma_c$ in the Landau gauge is the consequence of the relation for the renormalization constant for gluon-ghost-ghost vertex $Z_{Gcc} = Z_g \cdot Z_G^{1/2} \cdot Z_c$ that leads to $\gamma_{Gcc} = (\gamma_G + 2\gamma_c) - \beta_{\alpha_g}/(2\alpha_g)$. Since $\beta_{\alpha_g}(\alpha^*) = 0$ and in the Landau gauge $Z_{Gcc} = 1$, we have $\gamma_{Gcc} = 0$ and $\gamma_G + 2\gamma_c = 0$.

$$c^{(3)}_{\gamma_4} = \frac{8816623159}{133709346} - \frac{753675598}{2476099\sqrt{23}} + \frac{832\sqrt{2(931899\sqrt{23}-4436554)}\zeta_3}{6859\sqrt{107}} \tag{80}$$

$$- \frac{\sqrt{399093250633366162904063583977 1\sqrt{23} - 191396971644941833296265758811 70}}{164529350253\sqrt{4922}}. \tag{81}$$

Evaluating the coefficients in the Veneziano limit, we obtain

$$\gamma_H = \gamma_1 = -\gamma_2 = 0.21053\epsilon + 0.46247\epsilon^2 + 2.47105\epsilon^3, \tag{82}$$

$$\gamma_3 = 2.22982\epsilon + 3.88519\epsilon^2 + 20.5012\epsilon^3, \tag{83}$$

$$\gamma_4 = 1.68082\epsilon + 0.98321\epsilon^2 + 5.03949\epsilon^3. \tag{84}$$

One can see that all but $\gamma_2$ is positive for $\epsilon > 0$ and does not pose a problem to unitarity. Moreover, $\gamma_2 = -\gamma_H$ corresponds to the linear combination of operators[9] $O_{1-4}$ that vanish due to the equations of motion, while $\gamma_1 = \gamma_H$ corresponds to a linear combination of $O_{1-3}$ that becomes a descendant of $\mathrm{Tr}(H) + \mathrm{H.c.}$ when EOMs are imposed.

As for the finite-$N_c$ factors, we provide the following approximate expressions:

$$f^{(1)}_{\gamma_1,\gamma_2} = f^{(1)}_H, \qquad f^{(2)}_{\gamma_1,\gamma_2} = f^{(2)}_H, \qquad f^{(3)}_{\gamma_1,\gamma_2} = f^{(3)}_H, \tag{85}$$

$$\begin{aligned} f^{(1)}_{\gamma_3} &= \frac{N_c^4 - 0.751N_c^2 - 0.265}{N_c^4 - 5.392N_c^2 - 2.300}, \\ f^{(2)}_{\gamma_3} &= \frac{N_c^4 + 5.478N_c^2 - 0.150}{N_c^4 - 13.400N_c^2 + 45.771}, \\ f^{(3)}_{\gamma_3} &= \frac{N_c^4 + 27.974N_c^2 + 149.100}{N_c^4 - 15.762N_c^2 + 63.660}, \end{aligned} \tag{86}$$

$$\begin{aligned} f^{(1)}_{\gamma_4} &= \frac{N_c^4 - 0.397N_c^2 - 0.596}{N_c^4 - 5.265N_c^2 - 3.036}, \\ f^{(2)}_{\gamma_4} &= \frac{N_c^4 - 0.923N_c^2 + 3.520}{N_c^4 - 12.924N_c^2 + 42.288}, \\ f^{(3)}_{\gamma_4} &= \frac{N_c^4 + 10.300N_c^2 + 50.500}{N_c^4 - 15.454N_c^2 + 61.140}. \end{aligned} \tag{87}$$

The maximal value of MSE in these fits are $10^{-9}$, while the corresponding value for the ratio of two second-order polynomials (B4) reaches $4 \times 10^{-2}$.

[9]This fact can be deduced by considering the renormalization of local operator $[\delta S/\delta H]_R = Z_H^{1/2} \cdot (\delta S/\delta H)_0$.

## V. CONFORMAL WINDOW

In this section we investigate the size of the UV conformal window for the asymptotically safe theory with action equation (1) using perturbation theory.

### A. Constraints on the UV conformal window

We can find the UV conformal window directly from the expressions for fixed points and scaling exponents given in the previous sections. In the case when we retain only first three nonvanishing powers of $\epsilon$, we will call the bound on $\epsilon$ strict. The reason for this is that the higher-order ("subleading") coefficients in the power expansion (29) and (48) are not (yet) accurately determined due to the absence of higher loop terms in $\beta$ functions. This scheme is dictated first by the following constraints:

(i) perturbativity for couplings $0 < |\alpha^*| \lesssim 1$ [60];
(ii) vacuum stability $\alpha_u^* > 0$ and $\alpha_u^* + \alpha_v^* > 0$ [61]; and
(iii) no fixed-point merger [14] (the collision of the UV fixed point with an IR fixed point corresponds to $\theta = 0$).

The second strategy employs the approximation, where we retain subleading terms in $\epsilon$, so we refer to its bounds as subleading. There we also take into account all the above mentioned constraints from couplings, vacuum stability, and critical exponents.

### B. Investigation of the UV conformal window

The UV conformal window can be investigated using the above mentioned constraints. To do so, we first can equate the perturbative expressions for FP couplings to unity $(\alpha_u^* + \alpha_v^*)$ and scaling exponents to zero, and choose the smallest positive solution for $\epsilon$. Second, we can find the Padé approximants for these constraints and make the same manipulations. We represent our results as $\alpha^* = \epsilon P_{ij}$ and $\theta = \epsilon^2 P_{ij}$, where $P_{ij}$ are Padé approximants and $i + j = 2(3)$ for the strict (subleading) case. However, we cannot confidently trust the obtained results, because these approximants contain nonphysical poles. Nevertheless, they give tighter constraints on the conformal window and we provide all approximants that can be constructed from available series together with the corresponding bounds.

(i) From perturbative expansion of couplings (39)–(42), we note that the tightest bound on $\epsilon_{\mathrm{strict}}$ arises from

the gauge coupling. First, equating the gauge coupling to unity, we can find $\epsilon_{\text{strict}}$ and $\epsilon_{\text{subl}}$

$$\epsilon_{\text{strict}} \approx 0.457, \qquad \epsilon_{\text{subl}} \approx 0.363. \tag{88}$$

Second, we can construct the Padé approximants

$$\begin{aligned} P_{11}^{\alpha_g^*} &= \frac{0.456 - 3.081\epsilon}{1 - 8.467\epsilon}, \\ P_{12}^{\alpha_g^*} &= \frac{0.456 - 0.328\epsilon}{1 - 2.431\epsilon - 10.331\epsilon^2}, \\ P_{21}^{\alpha_g^*} &= \frac{0.456 - 0.885\epsilon + 3.760\epsilon^2}{1 - 3.651\epsilon} \end{aligned} \tag{89}$$

where the first line corresponds to the strict case, the second to subleading, and find the bounds

$$\epsilon_{\text{strict}_{11}} \approx 0.117, \qquad \epsilon_{\text{subl}_{12}} \approx 0.203, \qquad \epsilon_{\text{subl}_{21}} \approx 0.243. \tag{90}$$

(ii) In the same manner we can investigate the bounds arising from the vacuum stability condition [61]:

$$\epsilon_{\text{strict}} \approx 0.146, \qquad \epsilon_{\text{subl}} \approx 0.116. \tag{91}$$

To provide more stronger constrains for $\epsilon$, we use the Padé approximants:

$$\begin{aligned} P_{11}^{\alpha_u^*+\alpha_v^*} &= \frac{0.0625 - 0.719\epsilon}{1 - 8.438\epsilon}, \\ P_{12}^{\alpha_u^*+\alpha_v^*} &= \frac{0.625 - 0.673\epsilon}{1 - 7.695\epsilon + 2.281\epsilon^2}, \\ P_{21}^{\alpha_u^*+\alpha_v^*} &= \frac{0.625 - 0.656\epsilon - 0.194\epsilon^2}{1 - 7.425\epsilon}. \end{aligned} \tag{92}$$

The UV conformal window in this case is constrained as

$$\epsilon_{\text{strict}_{11}} \approx 0.087, \quad \epsilon_{\text{subl}_{12}} \approx 0.09287, \quad \epsilon_{\text{subl}_{21}} \approx 0.09272. \tag{93}$$

(iii) After the calculation of scaling exponents (58), we notice the behavior of $\theta_{2,3,4}$ with same-sign corrections at every order. However, the sign of leading $\epsilon^2$ coefficient for the relevant scaling exponent $\theta_1$ differs from other loop terms, which is the indication of possible FP merger. Thus, we can extract the constraints from the relevant scaling exponent, solving $\theta_1 = 0$:

$$\epsilon_{\text{strict}} \approx 0.249, \qquad \epsilon_{\text{subl}} \approx 0.234. \tag{94}$$

And using the Padé approximation

$$\begin{aligned} P_{11}^{\theta_1} &= \frac{0.608 - 6.681\epsilon}{1 - 9.826\epsilon}, \\ P_{12}^{\theta_1} &= \frac{0.608 - 1.717\epsilon}{1 - 0.661\epsilon + 9.495\epsilon^2}, \\ P_{21}^{\theta_1} &= \frac{0.608 - 1.129\epsilon - 6.455\epsilon^2}{1 - 0.695\epsilon}, \end{aligned} \tag{95}$$

we get

$$\epsilon_{\text{strict}_{11}} \approx 0.091, \quad \epsilon_{\text{subl}_{12}} \approx 0.354, \quad \epsilon_{\text{subl}_{21}} \approx 0.232. \tag{96}$$

It should be noted, that at 433 order we have only one fixed-point merger. However, if the subleading tendency continues in the 544 order, it will lead to the additional $\theta_3$ merger (57), which we do not study in this paper.

Moreover, we illustrate our results in Fig. 7. Here we show up the bounds for strict and subleading approaches (full lines) (88), (91), and (94), and their Padé approximants (dashed lines) that provide tightest constraints (90), (93), and (96) at 433 order. In addition, we add 211 and 322 orders for comparison. From these figures and from (88), (90), (91), (93), (94), and (96), we can deduce that the $\epsilon_{\text{subl}}$ bound is systematically tighter than the $\epsilon_{\text{strict}}$ bound, which arise from the last summands (39) and (55). The same situation was obtained at 322 order; see Ref. [13].

At the end, we demonstrate the size of the UV conformal window in Fig. 8. The left panel includes $\epsilon_{\text{strict}}$ bounds arising from vacuum stability (91) and (93). For

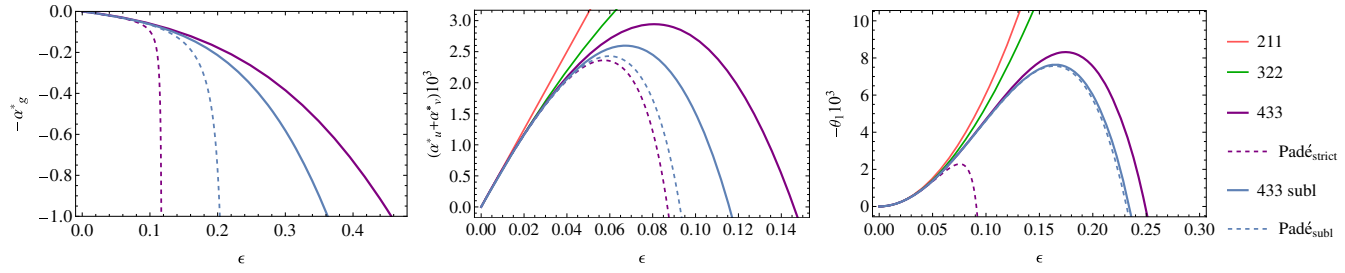


FIG. 7. $\epsilon_{\text{strict,subl}}$ bounds for 433 order (full lines) (88), (91), and (94), and their tighter Padé resummations (dashed lines) (90), (93), and (96). The 211 and 322 orders are also illustrated.

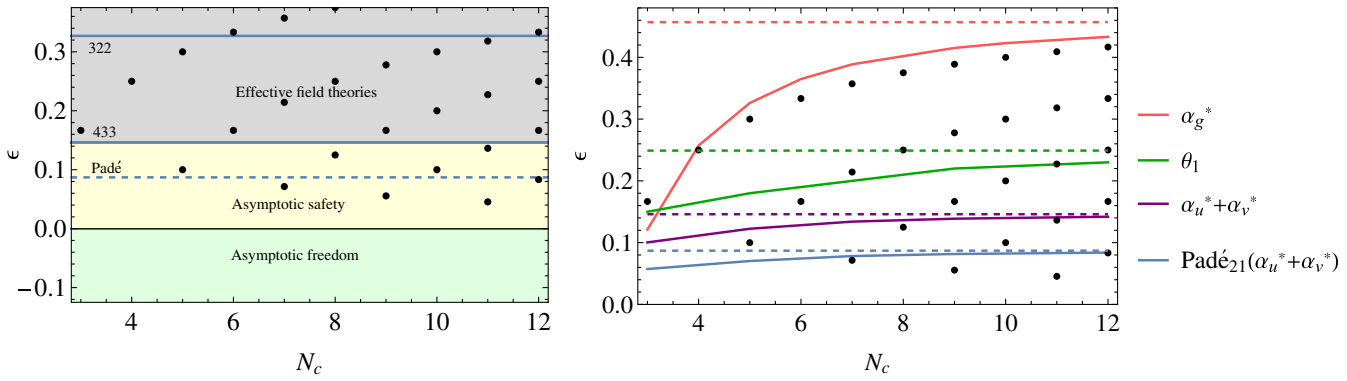


FIG. 8. Left panel: conformal window with asymptotic safety (yellow band), also showing regimes with asymptotic freedom (green) and effective theories (grey). Dots indicate the first few integer solutions (97) at 433 order. Moreover, this panel contains the new upper bound on $\epsilon$ at 433 order (91), and the tighter Padé approximant bound (dashed line) (93). Previous upper bounds at 322 [13] order also indicated. The right panel compares different schemes (88), (91), and (94) as given by $\epsilon_{\text{strict}}$. The dashed lines represent the asymptotic value; the full lines represent the upper boundary for the $\epsilon$ as functions of $N_c$.

comparison we have also indicated the previous bound at 322 order [13]. The right panel illustrates the boundaries for finite values of $N_c$. From this picture we can see that all constraints (88), (91), and (94) share roughly the same rate of convergence. In addition, it is clear that finite-$N_c$ corrections contract the conformal window (full lines) in comparison to infinite results (dashed lines).

Finally, using the tightest bound on the conformal window which is given by the vacuum instability $\epsilon_{\text{strict}} \approx 0.146$ (91), we obtain the smallest pair of integer values for $(N_c, N_f)$ compatible with asymptotic safety, which are indicated by black dots in Fig. 8. The first few integer solutions are

$$(N_c, N_f) = (5,28), (7,39), (8,45), (9,50), (10,56), (11,61), (11,62), (12,67)\ldots \tag{97}$$

### C. (De)stabilizing fluctuations

Following the ideas of Refs. [13,14], let us consider into which direction the higher loop corrections shift the beta functions. To do this we substitute the fixed points to order $O(\epsilon)^3$ back to the beta functions and take the series expansion in $\epsilon$ up to the first nonvanishing order. Keeping only highest available terms in RG functions, we obtain (cf., also Table II)

$$\begin{aligned}
\beta_g^{(4)}|_{322} &= -4.154\left(\frac{55.257+N_c^2}{-8.708+N_c^2}\right)\epsilon^5,\\
\beta_y^{(3)}|_{322} &= 1.263\left(\frac{33.923+N_c^2}{-8.442+N_c^2}\right)\epsilon^4,\\
\beta_u^{(3)}|_{322} &= -0.252\left(\frac{19.213+N_c^2}{-8.304+N_c^2}\right)\epsilon^4,\\
\beta_v^{(3)}|_{322} &= 0.213\left(\frac{83.582+N_c^2}{-8.514+N_c^2}\right)\epsilon^4.
\end{aligned} \tag{98}$$

Negative shifts to the beta functions ($\Delta\beta < 0$) are supposed to stabilize the UV fixed point [13,14], while $\Delta\beta > 0$, conversely, shift the zero towards larger values, which could even destabilize it. Thus, the obtained leading shifts for finite $N_c$ gives us a qualitative picture of the trend from higher-order loop contributions. It should be noted that these shifts have changed their signs compared to the previous results obtained in Refs. [13,14].

In the same manner, we insert the fixed points up to $\epsilon^3$ to the full available beta functions and find the subleading shifts for finite $N_c$ (see Table II with the Veneziano limit):

$$\begin{aligned}
\beta_g|_{433} &= 65.931\left(\frac{183.114+N_c^2}{-8.948+N_c^2}\right)\epsilon^6,\\
\beta_y|_{433} &= -11.143\left(\frac{75.486+N_c^2}{-8.946+N_c^2}\right)\epsilon^5,\\
\beta_u|_{433} &= 9.354\left(\frac{64.415+N_c^2}{-8.877+N_c^2}\right)\epsilon^5,\\
\beta_v|_{433} &= 47.863\left(\frac{51.740+N_c^2}{-7.993+N_c^2}\right)\epsilon^5.
\end{aligned} \tag{99}$$

We see that the results for $\beta_{g,y,u}$ change signs as compared to (98). However, they retained their behavior as in the case of Refs. [13,14]. Therefore, we can expect, that in the 544 order we will obtain similar results.

## VI. CONCLUSION

The availability of interacting UV fixed points in particle physics presents numerous prospects for constructing models; see, e.g., Ref. [20]. However, comprehending the size of the corresponding conformal window is equally crucial for any real-world applications. In this paper we investigated the Litim-Sannino model with action (1) at the 433 order. Extending the findings of [5,13,14] and confirming the results of [37], we have performed a full

search for interacting fixed points and computed scaling exponents and anomalous dimensions up to third order in the small parameter $\epsilon$ (4). It was also noted that their full expressions for finite $N_c$ are complicated; therefore, we performed fourth (second) order fits and provide the corresponding approximate expressions together. By comparing means square errors, we conclude that the ratio of fourth-order polynomials provide better approximation in certain cases; see, e.g., Fig. 6.

Moreover, we studied the size of the conformal window imposing conditions on the fixed-point values of the couplings and scaling exponents. We used different approximation orders and estimate the effect of subleading corrections. We compared various restrictions coming from the perturbativity of the strong coupling (88), vacuum instability (91), and possible fixed-point merger (94). Despite their qualitatively different origins, constraints are quantitatively similar, with vacuum stability offering the tightest bound (91). In addition, following Ref. [37] we tried to resum the $\epsilon$ series by means of Padé approximation and find that it gives even stronger constraints (90), (93), and (96). However, the presence of nonphysical poles in the approximants used to derive the bounds undermines our confidence in their accuracy. Perhaps this should be explored using other types of approximations and when high-order contributions in the 544 scheme will be available. We summarize our results in Fig. 8, where we illustrated the asymptotic safety regime together with the size of the UV conformal window. At the end, the asymptotically safe quantum field theories, which lie within the allowed conformal window, were also demonstrated in Eq. (97) and Fig. 8.

Furthermore, we notice that the authors of Ref. [37] mentioned that the anomalous dimension $\gamma_{m_\psi}$ of the fermion mass, which they computed in their paper, is *negative* to the leading order in $\epsilon$, while all the next-to-leading order terms are positive. Because of this, $\gamma_{m_\psi}$ can become negative and potentially pose a threat to unitarity [37]. We argue that this negative leading-order result is nothing else but the leading-order contribution to $(-\gamma_H)$. Positive higher-order terms computed in Ref. [37] cannot be trusted when evaluating scaling dimensions, since at the two-loop level the mixing comes into play. We account for this mixing in the present study and compute the anomalous-dimension matrix eigenvalues, one of which should be $(-\gamma_H)$ at any loop. But this is not the end of the story. We also argue that if EOMs are taken into account, the anomalous dimension matrix of dimension-three operators is modified $\gamma_O \to \tilde{\gamma}_O$ such that $\tilde{\gamma}_O$ has the same eigenvalues as $\gamma_O$ but with the flipped sign of the "dangerous" eigenvalue $(-\gamma_H) \to \gamma_H$. This can be anticipated and represents correct scaling of the operator that enters EOMs alongside with $O_4 \propto \partial^2 \mathrm{Tr}(H)$. Our analysis shows that all eigenvalues of the reduced anomalous dimension matrix are positive so dimension-three operators that break $G$ flavor symmetry do not spoil unitarity.

We believe that our findings can be used in a more elaborate analysis of the asymptotic safety in the Veneziano limit and beyond the latter. It is interesting how the results will be modified when the 544 order beta functions will be available, e.g., in connection with possible additional FP merger due to the potentially negative contribution of $\mathcal{O}(\epsilon^4)$ to $\theta_3$.

## ACKNOWLEDGMENTS

We thank Oleg Antipin, Nikita Lebedev, Georgy Kalagov, Dmitry Kazakov, Lukas Mizisin, and Vitaly Velizhanin for fruitful discussions. We also appreciate the correspondence with Tom Steudtner on Ref. [37] at the early stage of our study. The work of A. I. M was supported by the JINR Association of young scientists and specialists of Joint Institute for Nuclear Research (AYSS) Foundation, Project No. 24-301-02.

## APPENDIX A: RESULTS

In this appendix we provide complete expressions for the renormalization-group functions beyond the Veneziano limit. We follow [37] and introduce convenient abbreviations $\mathbf{r_c} \equiv N_c^{-2}$, $\mathbf{r_f} \equiv [(\frac{11}{2}+\epsilon)N_c]^{-2}$.

### 1. $\beta$ functions

The beta functions for rescaled coupling (3) read

$$\beta_g^{(1)}\alpha_g^{-2} = \frac{4\epsilon}{3}, \tag{A1}$$

$$\beta_g^{(2)}\alpha_g^{-2} = \left[25 + \frac{26\epsilon}{3} - (11+2\epsilon)\mathbf{r_c}\right]\alpha_g - \frac{1}{2}\alpha_y(11+2\epsilon)^2, \tag{A2}$$

$$\beta_g^{(3)}\alpha_g^{-2} = \left[\frac{6309+954\epsilon-224\epsilon^2}{54} + \frac{11(11+2\epsilon)(\epsilon-3)}{18}\mathbf{r_c} - \frac{11+2\epsilon}{4}\mathbf{r_c}^2\right]\alpha_g^2 - \frac{3}{8}(9-\mathbf{r_c})(11+2\epsilon)^2\alpha_g\alpha_y + \frac{1}{4}(11+2\epsilon)^2(3\epsilon+20)\alpha_y^2, \tag{A3}$$

$$\begin{aligned}\beta_g^{(4)}\alpha_g^{-2} &= \alpha_g^2\alpha_y\Big[\mathbf{r_c}^2\Big(\Big(18\zeta_3-\frac{3}{4}\Big)\epsilon^2+\Big(198\zeta_3-\frac{33}{4}\Big)\epsilon+\frac{1089\zeta_3}{2}-\frac{363}{16}\Big)\\
&+\mathbf{r_c}\Big(\Big(-54\zeta_3-\frac{1184}{9}\Big)\epsilon^2+\Big(-594\zeta_3-\frac{45749}{72}\Big)\epsilon-\frac{3267\zeta_3}{2}-\frac{161\epsilon^3}{18}-\frac{24079}{24}\Big)\\
&+\Big(36\zeta_3+\frac{8017}{36}\Big)\epsilon^2+\Big(396\zeta_3+\frac{38797}{72}\Big)\epsilon+1089\zeta_3+\frac{379\epsilon^3}{18}-\frac{12947}{48}\Big]\\
&+\alpha_g^3\Big[\mathbf{r_c}^3\Big(\frac{23\epsilon}{4}+\frac{253}{8}\Big)+\mathbf{r_c}^2\Big(\Big(\frac{623}{27}-\frac{488\zeta_3}{9}\Big)\epsilon^2+\Big(\frac{29753}{108}-\frac{5456\zeta_3}{9}\Big)\epsilon-1694\zeta_3+\frac{19613}{24}\Big)\\
&+\mathbf{r_c}\Big(\Big(\frac{128\zeta_3}{9}+\frac{7495}{243}\Big)\epsilon^2+\Big(\frac{2504\zeta_3}{9}+\frac{71765}{324}\Big)\epsilon+396\zeta_3+\frac{154\epsilon^3}{243}+\frac{30047}{72}\Big)\\
&+\Big(-\frac{56\zeta_3}{3}-\frac{21598}{243}\Big)\epsilon^2+\Big(-\frac{1808\zeta_3}{9}-\frac{123473}{324}\Big)\epsilon-550\zeta_3-\frac{260\epsilon^3}{243}-\frac{14731}{72}\Big]\\
&+\alpha_u^2\alpha_y[12\mathbf{r_c}+12\epsilon^2+132\epsilon+363]+48\alpha_u\alpha_v\alpha_y\mathbf{r_c}+\alpha_u\alpha_y^2\Big[-\mathbf{r_c}(10\epsilon+55)-10\epsilon^3-165\epsilon^2-\frac{1815\epsilon}{2}-\frac{6655}{4}\Big]\\
&-\alpha_v\alpha_y^2\mathbf{r_c}(20\epsilon+110)+12\alpha_v^2\alpha_y\mathbf{r_c}(\mathbf{r_f}+1)+\alpha_g\alpha_y^2\Big[\mathbf{r_c}\Big(\Big(12\zeta_3+\frac{89}{4}\Big)\epsilon^2+(132\zeta_3+154)\epsilon+363\zeta_3+\epsilon^3+\frac{5445}{16}\Big)\\
&+\Big(\frac{1659}{4}-12\zeta_3\Big)\epsilon^2+(2475-132\zeta_3)\epsilon-363\zeta_3+23\epsilon^3+\frac{78287}{16}\Big]\\
&+\alpha_y^3\Big[\mathbf{r_c}\Big(\Big(\frac{7}{3}-6\zeta_3\Big)\epsilon^2+\Big(\frac{77}{3}-66\zeta_3\Big)\epsilon-\frac{363\zeta_3}{2}+\frac{847}{12}\Big)-\frac{11\epsilon^4}{3}-100\epsilon^3-986\epsilon^2-\frac{25267\epsilon}{6}-\frac{105875}{16}\Big] \qquad \text{(A4)}\end{aligned}$$

$$\beta_y^{(1)}\alpha_y^{-1} = (13+2\epsilon)\alpha_y-6(1-\mathbf{r_c})\alpha_g, \qquad \text{(A5)}$$

$$\begin{aligned}\beta_y^{(2)}\alpha_y^{-1} &= -\frac{1}{8}[(11+2\epsilon)(2\epsilon+35)-32\mathbf{r_c}]\alpha_y^2+(1-\mathbf{r_c})(8\epsilon+49)\alpha_g\alpha_y+\frac{1}{6}(1-\mathbf{r_c})((20\epsilon-93)+9\mathbf{r_c})\alpha_g^2\\
&-4[(11+2\varepsilon)(1+\mathbf{r_f})]\alpha_y\alpha_u+4(1+\mathbf{r_f})\alpha_u^2+16\mathbf{r_f}\alpha_u\alpha_v-8\mathbf{r_f}\alpha_v\alpha_y(11+2\varepsilon)+4\mathbf{r_f}(1+\mathbf{r_f})\alpha_v^2 \qquad \text{(A6)}\end{aligned}$$

$$\begin{aligned}\beta_y^{(3)}\alpha_y^{-1} &= \alpha_g\alpha_y^2\Big[16\mathbf{r_c}^2+\mathbf{r_c}\Big(19\epsilon^2+\frac{445\epsilon}{2}+633\Big)-19\epsilon^2-\frac{445\epsilon}{2}-649\Big],\\
&+\alpha_g^2\alpha_y\Big[\mathbf{r_c}^2\Big(\Big(\frac{157}{8}-18\zeta_3\Big)\epsilon-81\zeta_3+\frac{721}{16}\Big)+\mathbf{r_c}((54\zeta_3+92)\epsilon+279\zeta_3+17\epsilon^2+31)\\
&+\Big(-36\zeta_3-\frac{893}{8}\Big)\epsilon-198\zeta_3-17\epsilon^2-\frac{1217}{16}\Big]\\
&+\alpha_g^3\Big[\frac{129\mathbf{r_c}^3}{4}+\mathbf{r_c}^2((23-24\zeta_3)\epsilon-132\zeta_3+62)+\mathbf{r_c}\Big(-\frac{70\epsilon^2}{27}-\frac{856\epsilon}{9}-\frac{2413}{12}\Big)+\Big(24\zeta_3+\frac{649}{9}\Big)\epsilon+132\zeta_3+\frac{70\epsilon^2}{27}+\frac{641}{6}\Big]\\
&+4\alpha_g\alpha_u\alpha_y(1-\mathbf{r_c})(\mathbf{r_f}+1)\Big(\epsilon+\frac{11}{2}\Big)\\
&+8\alpha_g\alpha_v\alpha_y\Big(\epsilon+\frac{11}{2}\Big)(1-\mathbf{r_c})\mathbf{r_f}+\alpha_u\alpha_y^2\Big[60\mathbf{r_c}+30\mathbf{r_f}\Big(\epsilon+\frac{11}{2}\Big)+12\epsilon^2+162\epsilon+528\Big]\\
&+\alpha_v\alpha_y^2\Big[24\mathbf{r_c}\mathbf{r_f}+48\mathbf{r_c}+60\mathbf{r_f}\Big(\epsilon+\frac{11}{2}\Big)\Big]+\alpha_y^3\Big[\mathbf{r_c}((6\zeta_3-28)\epsilon+39\zeta_3-162)-\frac{3\epsilon^3}{8}+\frac{59\epsilon^2}{16}+\frac{2595\epsilon}{32}+\frac{17413}{64}\Big]\\
&-\alpha_u^2\alpha_v(36\mathbf{r_f}+84)\mathbf{r_f}-\alpha_u\alpha_v^2(96\mathbf{r_f}+24)\mathbf{r_f}+\alpha_u\alpha_v\alpha_y[\mathbf{r_f}^2(80\epsilon+440)+\mathbf{r_f}(100\epsilon+490)]\\
&+\alpha_v^2\alpha_y\Big[\mathbf{r_f}^2\Big(85\epsilon+\frac{905}{2}\Big)+\mathbf{r_f}\Big(5\epsilon+\frac{25}{2}\Big)\Big]-\alpha_v^3(16\mathbf{r_f}^3+20\mathbf{r_f}^2+4\mathbf{r_f})-\alpha_u^3(32\mathbf{r_f}+8)\\
&+\alpha_u^2\alpha_y\Big[\mathbf{r_f}\Big(85\epsilon+\frac{905}{2}\Big)+5\epsilon+\frac{25}{2}\Big] \qquad \text{(A7)}\end{aligned}$$

$$\beta_u^{(1)} = 8\alpha_u^2 + 4\alpha_u\alpha_y - (11+2\epsilon)\alpha_y^2 + 24\alpha_u\alpha_v\mathbf{r_f}, \tag{A8}$$

$$\begin{aligned}\beta_u^{(2)} = {} & -24(1+5\mathbf{r_f})\alpha_u^3 - 16\alpha_y\alpha_u^2 - 352\alpha_u^2\alpha_v\mathbf{r_f} - 3(11+2\varepsilon)\alpha_y^2\alpha_u - 8\alpha_u\alpha_v^2\mathbf{r_f}(5+41\mathbf{r_f}) \\ & + 10(1-\mathbf{r_c})\alpha_g\alpha_y\alpha_u - 48\mathbf{r_f}\alpha_y\alpha_u\alpha_v - 2(11+2\varepsilon)(1-\mathbf{r_c})\alpha_g\alpha_y^2 + 4(11+2\varepsilon)\mathbf{r_f}\alpha_y^2\alpha_v + (11+2\varepsilon)^2\alpha_y^3\end{aligned} \tag{A9}$$

$$\begin{aligned}\beta_u^{(3)} = {} & \alpha_g^2\alpha_u\alpha_y\left[\mathbf{r_c}^2\left(36\zeta_3 - \frac{119}{4}\right) + \mathbf{r_c}\left(-36\zeta_3 + 8\epsilon + \frac{53}{2}\right) - 8\epsilon + \frac{13}{4}\right] \\ & + \alpha_g^2\alpha_y^2\left[\mathbf{r_c}^2\left(\left(\frac{131}{4} - 24\zeta_3\right)\epsilon - 132\zeta_3 + \frac{1441}{8}\right) + \mathbf{r_c}\left((24\zeta_3 - 66)\epsilon + 132\zeta_3 - 5\epsilon^2 - \frac{847}{4}\right)\right. \\ & \left. + 5\epsilon^2 + \frac{133\epsilon}{4} + \frac{253}{8}\right] + \alpha_g\alpha_v\alpha_y^2[\mathbf{r_c}\mathbf{r_f}((144\zeta_3 - 112)\epsilon + 792\zeta_3 - 616) + \mathbf{r_f}((112 - 144\zeta_3)\epsilon - 792\zeta_3 + 616)] \\ & - \alpha_v\alpha_y^3\left[\mathbf{r_c}(96\zeta_3 + 152) - 64\mathbf{r_f}\left(\epsilon + \frac{11}{2}\right)\right] + \alpha_g\alpha_u^2\alpha_y(1-\mathbf{r_c})(96\zeta_3 - 102) \\ & + \alpha_g\alpha_u\alpha_y^2\left[\mathbf{r_c}\left(\left(120\zeta_3 - \frac{149}{2}\right)\epsilon + 660\zeta_3 - \frac{1639}{4}\right) + \left(\frac{149}{2} - 120\zeta_3\right)\epsilon - 660\zeta_3 + \frac{1639}{4}\right] \\ & + \alpha_g\alpha_y^3\left[\mathbf{r_c}\left((5 - 24\zeta_3)\epsilon^2 + (55 - 264\zeta_3)\epsilon - 726\zeta_3 + \frac{605}{4}\right) + (24\zeta_3 - 5)\epsilon^2 + (264\zeta_3 - 55)\epsilon + 726\zeta_3 - \frac{605}{4}\right] \\ & + \alpha_u\alpha_y^3\left[\mathbf{r_c}(12\zeta_3 - 168) - \frac{315\epsilon^2}{4} - \frac{3209\epsilon}{4} - \frac{32483}{16}\right] \\ & + \alpha_y^4\left[\mathbf{r_c}((20 - 24\zeta_3)\epsilon - 132\zeta_3 + 110) + \frac{13\epsilon^3}{4} + \frac{265\epsilon^2}{8} + \frac{1111\epsilon}{16} - \frac{2541}{32}\right] + \alpha_u\alpha_v^2\alpha_y[642\mathbf{r_f}^2 + 66\mathbf{r_f}] \\ & + \alpha_g\alpha_u\alpha_v\alpha_y\left[-\frac{9}{2}\mathbf{r_f}(-4 + \mathbf{r_f}(11+2\epsilon)^2)(-17 + 16\zeta_3)\right] \\ & + \alpha_u^3\alpha_v[\mathbf{r_f}^2(6144\zeta_3 + 6752) + \mathbf{r_f}(1536\zeta_3 + 2912)] - \alpha_u^2\alpha_v^2[280\mathbf{r_f} - \mathbf{r_f}^2(9216\zeta_3 + 12728)] \\ & + \alpha_v^2\alpha_y^2[\mathbf{r_f}^2((216\zeta_3 + 136)\epsilon + 1188\zeta_3 + 748) + \mathbf{r_f}(64\epsilon + 352)] \\ & - \alpha_u\alpha_v^3[-(\mathbf{r_f}^3(5376\zeta_3 + 6568)) - \mathbf{r_f}^2(768\zeta_3 + 1472) + 104\mathbf{r_f}] \\ & + \alpha_u^3\alpha_y(226\mathbf{r_f} + 34) + 648\alpha_u^2\alpha_v\alpha_y\mathbf{r_f} + \alpha_u^4[\mathbf{r_f}(1152\zeta_3 + 2360) + 104] \\ & + \alpha_u^2\alpha_y^2[\mathbf{r_f}((216\zeta_3 + 156)\epsilon + 1188\zeta_3 + 858) + 166\epsilon + 889] \\ & + \alpha_u\alpha_v\alpha_y^2\mathbf{r_f}((192\zeta_3 + 734)\epsilon + 1056\zeta_3 + 3965)\end{aligned} \tag{A10}$$

$$\beta_v^{(1)} = 12\alpha_u^2 + 16\alpha_u\alpha_v + 4\alpha_v\alpha_y + 4(1+4\mathbf{r_f})\alpha_v^2, \tag{A11}$$

$$\begin{aligned}\beta_v^{(2)} = {} & -24\alpha_v^3\mathbf{r_f}(3+7\mathbf{r_f}) - 8(1+4\mathbf{r_f})\alpha_y\alpha_v^2 - 352\alpha_u\alpha_v^2\mathbf{r_f} - (11+2\varepsilon)(3\alpha_v - 4\alpha_u)\alpha_y^2 - 8(5+41\mathbf{r_f})\alpha_u^2\alpha_v \\ & + 10(1-\mathbf{r_c})\alpha_g\alpha_y\alpha_v - 32\alpha_y\alpha_u\alpha_v - 24\alpha_y\alpha_u^2 + (11+2\varepsilon)^2\alpha_y^3 - 96\alpha_u^3\end{aligned} \tag{A12}$$

$$\begin{aligned}\beta_v^{(3)} &= 192\alpha_u^3\alpha_y + \alpha_y^4\left[-10\epsilon^3 - 183\epsilon^2 - \frac{2211\epsilon}{2} - \frac{8833}{4}\right] + \alpha_g^2\alpha_v\alpha_y\left[\mathbf{r_c}^2\left(36\zeta_3 - \frac{119}{4}\right) + \mathbf{r_c}\left(-36\zeta_3 + 8\epsilon + \frac{53}{2}\right) - 8\epsilon + \frac{13}{4}\right]\\
&+ \alpha_g^2\alpha_y^2(1-\mathbf{r_c})(24\epsilon^2 + 264\epsilon + 726) + \alpha_g\alpha_u^2\alpha_y(1-\mathbf{r_c})(144\zeta_3 - 153) + \alpha_g\alpha_u\alpha_v\alpha_y(1-\mathbf{r_c})(192\zeta_3 - 204)\\
&+ \alpha_g\alpha_u\alpha_y^2(1-\mathbf{r_c})[(112 - 144\zeta_3)\epsilon - 792\zeta_3 + 616] + \alpha_g\alpha_v\alpha_y^2(1-\mathbf{r_c})\left[\left(\frac{149}{2} - 120\zeta_3\right)\epsilon - 660\zeta_3 + \frac{1639}{4}\right]\\
&+ \alpha_g\alpha_y^3\left[\mathbf{r_c}\left((2 - 24\zeta_3)\epsilon^2 + (22 - 264\zeta_3)\epsilon - 726\zeta_3 + \frac{121}{2}\right) + (24\zeta_3 - 2)\epsilon^2 + (264\zeta_3 - 22)\epsilon + 726\zeta_3 - \frac{121}{2}\right]\\
&+ \alpha_v\alpha_y^3\left[\mathbf{r_c}(12\zeta_3 - 136) - \frac{187\epsilon^2}{4} - \frac{1801\epsilon}{4} - \frac{16995}{16}\right] + \alpha_v^3\alpha_y(322\mathbf{r_f}^2 + 130\mathbf{r_f})\\
&+ \alpha_g\alpha_v^2\alpha_y\Big[\mathbf{r_f}^2((204 - 192\zeta_3)\epsilon^2 + (2244 - 2112\zeta_3)\epsilon - 5808\zeta_3 + 6171)\\
&+ \mathbf{r_f}\left((51 - 48\zeta_3)\epsilon^2 + (561 - 528\zeta_3)\epsilon - 1260\zeta_3 + \frac{5355}{4}\right) + 48\zeta_3 - 51\Big]\\
&+ \alpha_u^2\alpha_v^2[\mathbf{r_f}^2(8064\zeta_3 + 10476) + \mathbf{r_f}(1152\zeta_3 + 6680) + 12] + \alpha_u\alpha_v^3[\mathbf{r_f}^2(6144\zeta_3 + 10544) + 1264\mathbf{r_f}]\\
&+ \alpha_v^4[\mathbf{r_f}^3(2112\zeta_3 + 2960) + \mathbf{r_f}^2(960\zeta_3 + 1844) + 132\mathbf{r_f}] + \alpha_u^2\alpha_v\alpha_y(642\mathbf{r_f} + 66) + 648\alpha_u\alpha_v^2\alpha_y\mathbf{r_f}\\
&+ \alpha_u^4[\mathbf{r_f}(1536\zeta_3 + 1700) + 384\zeta_3 + 772] + \alpha_u^3\alpha_v[\mathbf{r_f}(4608\zeta_3 + 9600) + 480]\\
&+ \alpha_u\alpha_v\alpha_y^2[\mathbf{r_f}((528\zeta_3 + 132)\epsilon + 2904\zeta_3 + 726) + (96\zeta_3 + 152)\epsilon + 528\zeta_3 + 788]\\
&+ \alpha_v^2\alpha_y^2\left[\mathbf{r_f}((192\zeta_3 + 268)\epsilon + 1056\zeta_3 + 1426) + 41\epsilon + \frac{427}{2}\right] + \alpha_u^2\alpha_y^2\left[(192\zeta_3 + 187)\epsilon + 1056\zeta_3 + \frac{1985}{2}\right]\\
&+ \alpha_u\alpha_y^3[(-96\zeta_3 - 88)\epsilon^2 + (-1056\zeta_3 - 904)\epsilon - 2904\zeta_3 - 2310]. \qquad \text{(A13)}\end{aligned}$$

### 2. Anomalous dimension of fields and scalar mass squared

The gauge-independent scalar field anomalous dimension reads

$$\gamma_H^{(1)} = \alpha_y, \qquad \text{(A14)}$$

$$\gamma_H^{(2)} = 2\alpha_u^2(\mathbf{r_f} + 1) - \frac{5}{2}\alpha_y\alpha_g(\mathbf{r_c} - 1) - \frac{3}{4}\alpha_y^2(2\epsilon + 11) + 8\alpha_u\alpha_v\mathbf{r_f} + 2\alpha_v^2\mathbf{r_f}(\mathbf{r_f} + 1), \qquad \text{(A15)}$$

$$\begin{aligned}\gamma_H^{(3)} &= -4\alpha_u^3(4\mathbf{r_f} + 1) + \alpha_y\left(-\frac{15}{2}(\mathbf{r_f} + 1)\alpha_u^2 - 30\mathbf{r_f}\alpha_u\alpha_v - \frac{15}{2}\mathbf{r_f}(\mathbf{r_f} + 1)\alpha_v^2\right)\\
&\times \alpha_y^2\left(\frac{5}{2}(\mathbf{r_f} + 1)(2\epsilon + 11)\alpha_u + 5\mathbf{r_f}(2\epsilon + 11)\alpha_v\right) + \alpha_y^3\left(3\zeta_3\mathbf{r_c} - 2\mathbf{r_c} + \frac{1}{64}(2\epsilon + 11)(10\epsilon + 183)\right)\\
&+ \alpha_g\alpha_y^2\frac{1}{16}(48\zeta_3 - 5)(\mathbf{r_c} - 1)(2\epsilon + 11) + \frac{1}{16}\alpha_g^2\alpha_y(\mathbf{r_c} - 1)(144\zeta_3\mathbf{r_c} - 119\mathbf{r_c} + 32\epsilon - 13)\\
&- 12\alpha_u\alpha_v^2\mathbf{r_f}(4\mathbf{r_f} + 1) - 6\alpha_u^2\alpha_v\mathbf{r_f}(3\mathbf{r_f} + 7) - 2\alpha_v^3\mathbf{r_f}(\mathbf{r_f} + 1)(4\mathbf{r_f} + 1). \qquad \text{(A16)}\end{aligned}$$

The scalar mass term respects $U_L(N_f) \times U_R(N_f)$ global symmetry and its anomalous dimension is given by

$$\gamma_{m^2}^{(1)} = 8\alpha_u + 4\alpha_v + 2\alpha_y, \qquad \text{(A17)}$$

$$\gamma_{m^2}^{(2)} = -20(\alpha_u^2 - \mathbf{r_f}) - 8\alpha_v\alpha_y(1 + \mathbf{r_f}) - 16\alpha_u\alpha_y + 5\alpha_g\alpha_y(1 - \mathbf{r_c}) - \frac{3}{2}\alpha_y^2(11 + 2\epsilon) - 20\alpha_v^2\mathbf{r_f}(1 + \mathbf{r_f}) - 80\alpha_u\alpha_v\mathbf{r_f}, \qquad \text{(A18)}$$

$$\gamma_{m^2}^{(3)} = \alpha_u^3(888\mathbf{r_f}+240)+\alpha_u^2\alpha_v(984\mathbf{r_f}^2+2388\mathbf{r_f}+12)+\alpha_y((33\mathbf{r_f}^2+33\mathbf{r_f})\alpha_v^2+(33\mathbf{r_f}+33)\alpha_u^2+132\mathbf{r_f}\alpha_u\alpha_v)$$
$$+\alpha_y^2\Bigg[\alpha_u(264\zeta_3+264\zeta_3\mathbf{r_f}+48\zeta_3\mathbf{r_f}\epsilon-6\mathbf{r_f}\epsilon-33\mathbf{r_f}+48\zeta_3\epsilon+76\epsilon+394)$$
$$+\alpha_v\left(528\zeta_3\mathbf{r_f}+96\zeta_3\mathbf{r_f}\epsilon+29\mathbf{r_f}\epsilon+\frac{295\mathbf{r_f}}{2}+41\epsilon+\frac{427}{2}\right)\Bigg]$$
$$+\alpha_g\alpha_y[\alpha_v(48\zeta_3-48\zeta_3\mathbf{r_c}-48\zeta_3\mathbf{r_c}\mathbf{r_f}+51\mathbf{r_c}\mathbf{r_f}+51\mathbf{r_c}+48\zeta_3\mathbf{r_f}-51\mathbf{r_f}-51)+\alpha_u(96\zeta_3-96\zeta_3\mathbf{r_c}+102\mathbf{r_c}-102)]$$
$$+\alpha_y^3\left(30\zeta_3\mathbf{r_c}-24\mathbf{r_c}-\frac{187\epsilon^2}{8}-\frac{1801\epsilon}{8}-\frac{16995}{32}\right)$$
$$+\alpha_g\alpha_y^2\left(-330\zeta_3+330\zeta_3\mathbf{r_c}+60\zeta_3\mathbf{r_c}\epsilon-\frac{149\mathbf{r_c}\epsilon}{4}-\frac{1639\mathbf{r_c}}{8}-60\zeta_3\epsilon+\frac{149\epsilon}{4}+\frac{1639}{8}\right)$$
$$+\alpha_g^2\alpha_y\left(18\zeta_3\mathbf{r_c}^2-\frac{119\mathbf{r_c}^2}{8}-18\zeta_3\mathbf{r_c}+4\mathbf{r_c}\epsilon+\frac{53\mathbf{r_c}}{4}-4\epsilon+\frac{13}{8}\right)$$
$$+\alpha_u\alpha_v^2(2664\mathbf{r_f}^2+720\mathbf{r_f})+\alpha_v^3(444\mathbf{r_f}^3+564\mathbf{r_f}^2+120\mathbf{r_f}). \tag{A19}$$

The anomalous dimensions of fermion ($\gamma_\psi$), gluon ($\gamma_G$), and ghost ($\gamma_c$) fields depend on the gauge-fixing parameter $\xi$. The results up to three-loop level are given by

$$\gamma_\psi^{(1)} = \frac{1}{4}\alpha_y(2\epsilon+11)-\frac{1}{2}\xi\alpha_g(\mathbf{r_c}-1), \tag{A20}$$

$$\gamma_\psi^{(2)} = -\frac{1}{8}\alpha_g^2(\mathbf{r_c}-1)(\xi(8+\xi)+3\mathbf{r_c}-4\epsilon)+\frac{1}{2}\alpha_g\alpha_y(\mathbf{r_c}-1)(2\epsilon+11)+-\frac{1}{32}\alpha_y^2(2\epsilon+11)(2\epsilon+23), \tag{A21}$$

$$\gamma_\psi^{(3)} = -\frac{11}{8}\alpha_u^2\alpha_y(\mathbf{r_f}+1)(2\epsilon+11)+\alpha_y^2\left(\left(2\mathbf{r_c}+\frac{1}{2}(2\epsilon+11)^2\right)\alpha_u+4\mathbf{r_c}\alpha_v\right)$$
$$\times\frac{1}{256}\alpha_y^3(2\epsilon+11)(192\zeta_3\mathbf{r_c}-128\mathbf{r_c}+4(41-3\epsilon)\epsilon+1217)$$
$$-\frac{1}{32}\alpha_g\alpha_y^2(\mathbf{r_c}-1)(2\epsilon+11)(48\zeta_3+24\epsilon+137)+\frac{1}{64}\alpha_g^2\alpha_y(\mathbf{r_c}-1)(2\epsilon+11)(48\zeta_3(\mathbf{r_c}+4)-51\mathbf{r_c}-12\epsilon-77)$$
$$+\frac{1}{576}\alpha_g^3[-160\epsilon^2(\mathbf{r_c}-1)+24\epsilon(\mathbf{r_c}-1)(109+9\mathbf{r_c})-90\xi^3(\mathbf{r_c}-1)-27\xi^2(\mathbf{r_c}-1)(13+4\zeta_3)$$
$$-18(\mathbf{r_c}-1)(-331+208\mathbf{r_c}+6\mathbf{r_c}^2-6(7+16\mathbf{r_c})\zeta_3)+\xi(612\epsilon(\mathbf{r_c}-1)-27(\mathbf{r_c}-1)(-37+8\zeta_3))]$$
$$-\frac{11}{2}\alpha_u\alpha_v\alpha_y\mathbf{r_f}(2\epsilon+11)-\frac{11}{8}\alpha_v^2\alpha_y\mathbf{r_f}(\mathbf{r_f}+1)(2\epsilon+11) \tag{A22}$$

$$\gamma_G^{(1)} = \frac{1}{6}\alpha_g(3\xi+4\epsilon+9), \tag{A23}$$

$$\gamma_G^{(2)} = -\frac{1}{8}\alpha_g^2(-11\xi-2\xi^2+\mathbf{r_c}(8\epsilon+44)-28\epsilon-95)-\alpha_g\alpha_y\frac{1}{4}(2\epsilon+11)^2, \tag{A24}$$

$$\gamma_G^{(3)} = \frac{1}{8}\alpha_g\alpha_y^2(2\epsilon+11)^2(3\epsilon+20)+\frac{1}{32}\alpha_g^2\alpha_y(6\mathbf{r_c}-31)(2\epsilon+11)^2$$
$$+\frac{1}{288}\alpha_g^3[-81\xi-27\xi^2(11+2\zeta_3)-63\xi^3-36\mathbf{r_c}^2(2\epsilon+11)-54\zeta_3(-4\xi+16\mathbf{r_c}(2\epsilon+11)+16\epsilon+85)$$
$$+2\mathbf{r_c}(2\epsilon+11)(44\epsilon+273)-4\epsilon(72\xi+196\epsilon+347)+6117] \tag{A25}$$

$$\gamma_c^{(1)} = \frac{1}{4}\alpha_g(\xi-3), \tag{A26}$$

$$\gamma_c^{(2)} = \frac{1}{48}\alpha_g^2(-3\xi + 20\epsilon + 15), \tag{A27}$$

$$\begin{aligned}\gamma_c^{(3)} = &-\alpha_g^2\alpha_y\frac{23}{64}(2\epsilon+11)^2 \\ &+\frac{1}{1728}\alpha_g^3[81\xi^3 - 162\xi^2(-1+\zeta_3) - 108\xi(7\epsilon + 6(5+\zeta_3)) \\ &+ 12\epsilon(983 + 216\zeta_3 + 27\mathbf{r_c}(-15+16\zeta_3)) + 560\epsilon^2 + 9(3569 + 1530\zeta_3 + 198\mathbf{r_c}(-15+16\zeta_3))].\end{aligned} \tag{A28}$$

### 3. Anomalous dimensions for dimension-three operators

Here we collect the matrix elements of the $4\times 4$ anomalous dimension for a set of dimension-three operators. Note that we assume that the operators are rescaled according to Eq. (7):

$$(\gamma_O^{(1)})_{11} = -3\alpha_g(1-\mathbf{r_c}) + \frac{\alpha_y}{2}(11+2\epsilon), \tag{A29}$$

$$(\gamma_O^{(2)})_{11} = 2\alpha_g\alpha_y(11+2\epsilon)(1-\mathbf{r_c}) + \frac{\alpha_g^2}{12}(1-\mathbf{r_c})(9\mathbf{r_c} + 20\epsilon - 93) + \alpha_y^2\left[2\mathbf{r_c} - \frac{1}{4}\epsilon(\epsilon+17) - \frac{253}{16}\right], \tag{A30}$$

$$\begin{aligned}(\gamma_O^{(3)})_{11} = &\alpha_g^2\alpha_y\left[\frac{9}{2}(11+2\epsilon)(1-\mathbf{r_c})(\mathbf{r_c}-2)\zeta_3 - \frac{1-\mathbf{r_c}}{32}(2\epsilon(157\mathbf{r_c} + 136\epsilon + 861) + 959\mathbf{r_c} + 1243)\right] \\ &+\alpha_g^3\left[6(11+2\epsilon)(1-\mathbf{r_c}^2)\zeta_3 - \frac{1-\mathbf{r_c}}{216}(27(92\epsilon+377)\mathbf{r_c} + 3483\mathbf{r_c}^2 - 4\epsilon(70\epsilon+1947) - 11538)\right] \\ &+\alpha_g\alpha_y^2\left[3(11+2\epsilon)(1-\mathbf{r_c})\zeta_3 - \frac{1-\mathbf{r_c}}{16}(128\mathbf{r_c} + 2\epsilon(76\epsilon+895) + 5247)\right] - 11\alpha_u\alpha_v\alpha_y(11+2\epsilon)\mathbf{r_f} \\ &+\alpha_u\alpha_y^2((11+2\epsilon)^2 + 12\mathbf{r_c}) - \frac{11\alpha_v^2\alpha_y}{4}(11+2\epsilon)(1+\mathbf{r_f})\mathbf{r_f} + \alpha_v\alpha_y^2(4\mathbf{r_c}(\mathbf{r_f}+3)) \\ &+\alpha_y^3\left[\frac{3}{2}(11+2\epsilon)\mathbf{r_c}\zeta_3 - \frac{11+2\epsilon}{128}(4\epsilon(3\epsilon-41) - 1217) - (14\epsilon+79)\mathbf{r_c}\right] - \frac{11(11+2\epsilon)(1+\mathbf{r_f})}{4}\alpha_u^2\alpha_y,\end{aligned} \tag{A31}$$

$$(\gamma_O^{(1)})_{12}\cdot\alpha_y^{-3/2} = -4(11+2\epsilon), \tag{A32}$$

$$(\gamma_O^{(2)})_{12}\cdot\alpha_y^{-3/2} = -8(11+2\epsilon)(1-\mathbf{r_c})\alpha_g + 8\alpha_v(11+2\epsilon)\mathbf{r_f} + 4(11+2\epsilon)^2\alpha_y, \tag{A33}$$

$$\begin{aligned}(\gamma_O^{(3)})_{12}\cdot\alpha_y^{-3/2} = &\alpha_g^2(11+2\epsilon)(1-\mathbf{r_c})\left[48\zeta_3\mathbf{r_c} + \frac{1}{2}(-131\mathbf{r_c} + 20\epsilon + 23)\right] + \alpha_g\alpha_u(11+2\epsilon)(1-\mathbf{r_c})[72 - 96\zeta_3] \\ &+\alpha_y^2(11+2\epsilon)\left[\frac{1}{8}(320\mathbf{r_c} + 4\epsilon(13\epsilon+61) - 231) - 48\zeta_3\mathbf{r_c}\right] + \alpha_g\alpha_y(11+2\epsilon)^2(1-\mathbf{r_c})[24\zeta_3 - 5] \\ &+\alpha_g\alpha_v(11+2\epsilon)(1-\mathbf{r_c})\mathbf{r_f}[112 - 144\zeta_3] + \alpha_v^2(11+2\epsilon)\mathbf{r_f}[96\zeta_3\mathbf{r_f} + 32(5\mathbf{r_f}+2)] \\ &+\alpha_u^2(11+2\epsilon)[96\zeta_3\mathbf{r_f} + 32(5\mathbf{r_f}+2)] + \alpha_u\alpha_v(11+2\epsilon)\mathbf{r_f}[96\zeta_3 + 480] \\ &-\alpha_u\alpha_y[96\zeta_3\mathbf{r_c} + 2(180\mathbf{r_c} + 4\epsilon(25\epsilon+263) + 2761)] + \alpha_v\alpha_y[64((11+2\epsilon)\mathbf{r_f} - 6\mathbf{r_c}) - 288\zeta_3\mathbf{r_c}],\end{aligned} \tag{A34}$$

$$(\gamma_O^{(2)})_{13}\cdot\alpha_y^{-3/2} = 4(11+2\epsilon)^2(\alpha_y + 2\alpha_u), \tag{A35}$$

$$(\gamma_O^{(3)})_{13}\cdot\alpha_y^{-3/2} = 96(11+2\epsilon)\alpha_u^2(1+\zeta_3)+\alpha_g\alpha_u(11+2\epsilon)(1-\mathbf{r_c})(112-144\zeta_3) + \alpha_g\alpha_v(11+2\epsilon)(1-\mathbf{r_c})(72-96\zeta_3)+\alpha_g\alpha_y(11+2\epsilon)^2(1-\mathbf{r_c})(24\zeta_3-2) + \alpha_u\alpha_v(11+2\epsilon)[48\zeta_3(5\mathbf{r_f}+1)+16(11\mathbf{r_f}-1)]+24\alpha_g^2(11+2\epsilon)^2(1-\mathbf{r_c}) - \alpha_u\alpha_y(11+2\epsilon)[72(11+2\epsilon)\zeta_3+4(22\epsilon+105)]+96\alpha_v^2(11+2\epsilon)\mathbf{r_f}(1+\zeta_3) - \alpha_v\alpha_y[96\zeta_3\mathbf{r_c}+8(32\mathbf{r_c}+12\epsilon(\epsilon+10)+297)]-(11+2\epsilon)^2(10\epsilon+73)\alpha_y^2, \tag{A36}$$

$$(\gamma_O^{(2)})_{21}\cdot\alpha_y^{-3/2} = -\frac{(11+2\epsilon)(1+\mathbf{r_f})}{2}, \tag{A37}$$

$$(\gamma_O^{(3)})_{21}\cdot\alpha_y^{-3/2} = \frac{\alpha_g}{4}(11+2\epsilon)(1-\mathbf{r_c})(1+\mathbf{r_f})+\alpha_u(11+2\epsilon)(1+6\mathbf{r_f})+\frac{\alpha_v}{2}(11+2\epsilon)\mathbf{r_f}(9+5\mathbf{r_f}) + \frac{\alpha_y}{8}[36\mathbf{r_c}+4\epsilon(5\mathbf{r_f}+\epsilon+16)+110\mathbf{r_f}+231], \tag{A38}$$

$$(\gamma_O^{(1)})_{22} = 3\alpha_y+8\alpha_u+12\mathbf{r_f}\alpha_v, \tag{A39}$$

$$(\gamma_O^{(2)})_{22} = -16\alpha_u\alpha_y+\frac{15\alpha_g\alpha_y}{2}(1-\mathbf{r_c})-248\mathbf{r_f}\alpha_u\alpha_v-24\mathbf{r_f}\alpha_v\alpha_y - 2\alpha_u^2(61\mathbf{r_f}+13)-6\alpha_v^2(19\mathbf{r_f}+3)\mathbf{r_f}-\frac{9\alpha_y^2}{4}(11+2\epsilon), \tag{A40}$$

$$(\gamma_O^{(3)})_{22} = \alpha_g\alpha_u\alpha_y(1-\mathbf{r_c})(96\zeta_3-102)-\alpha_g^2\alpha_y(1-\mathbf{r_c})\left[27\zeta_3\mathbf{r_c}-\frac{3}{16}(119\mathbf{r_c}-32\epsilon+13)\right] + \alpha_g\alpha_v\alpha_y(1-\mathbf{r_c})\mathbf{r_f}(144\zeta_3-153)+\alpha_g\alpha_y^2(11+2\epsilon)(1-\mathbf{r_c})\left[\frac{303}{16}-33\zeta_3\right]+454\mathbf{r_f}\alpha_u\alpha_v\alpha_y + \alpha_u^2\alpha_v[1152\zeta_3\mathbf{r_f}(4\mathbf{r_f}+1)+2\mathbf{r_f}(2511\mathbf{r_f}+1195)]+\alpha_u^3[1152\zeta_3\mathbf{r_f}+108(22\mathbf{r_f}+1)] + \alpha_u\alpha_v^2\mathbf{r_f}[4608\zeta_3\mathbf{r_f}+140(50\mathbf{r_f}-1)]+\alpha_u\alpha_y^2\left[84(11+2\epsilon)\zeta_3\mathbf{r_f}+\left(71\epsilon+\frac{781}{2}\right)\mathbf{r_f}+129\epsilon+\frac{1371}{2}\right] + \alpha_v^3\mathbf{r_f}[192\zeta_3(7\mathbf{r_f}+1)\mathbf{r_f}+6(7\mathbf{r_f}(46\mathbf{r_f}+15)-9)]+\alpha_v\alpha_y^2\mathbf{r_f}\left[48(11+2\epsilon)\zeta_3+\frac{3}{2}(166\epsilon+889)\right] - \alpha_y^3\left[\frac{3}{64}(11+2\epsilon)(310\epsilon+1321)+(76-33\zeta_3)\mathbf{r_c}\right]+\frac{\alpha_u^2\alpha_y}{2}(83+467\mathbf{r_f})+\frac{3\alpha_v^2\alpha_y}{2}\mathbf{r_f}(17+145\mathbf{r_f}), \tag{A41}$$

$$(\gamma_O^{(1)})_{23} = 12\alpha_u+8\alpha_v, \tag{A42}$$

$$(\gamma_O^{(2)})_{23} = -16\alpha_v\alpha_y-24\alpha_u\alpha_y+2(11+2\epsilon)\alpha_y^2-96\alpha_u^2-112\mathbf{r_f}\alpha_v^2-24(1+9\mathbf{r_f})\alpha_u\alpha_v, \tag{A43}$$

$$(\gamma_O^{(3)})_{23} = \alpha_g\alpha_u\alpha_y(1-\mathbf{r_c})[144\zeta_3-153]+192\alpha_u^2\alpha_y+\alpha_g\alpha_v\alpha_y(1-\mathbf{r_c})[96\zeta_3-102] + \alpha_g\alpha_y^2(11+2\epsilon)(1-\mathbf{r_c})(28-36\zeta_3)+\alpha_u^2\alpha_v[3456\zeta_3\mathbf{r_f}+8(901\mathbf{r_f}+31)] + \alpha_u^3[384\zeta_3(4\mathbf{r_f}+1)+1700\mathbf{r_f}+772]+\alpha_u\alpha_v^2\mathbf{r_f}[576\zeta_3(7\mathbf{r_f}+1)+4(1233\mathbf{r_f}+769)] + \alpha_u\alpha_y^2\left[72(11+2\epsilon)\zeta_3+139\epsilon+\frac{1457}{2}\right]+\alpha_v^3\mathbf{r_f}[1536\zeta_3\mathbf{r_f}+8(259\mathbf{r_f}+47)] + \alpha_v\alpha_y^2[12(11+2\epsilon)\zeta_3(8\mathbf{r_f}+1)+2\epsilon(8\mathbf{r_f}+37)+88\mathbf{r_f}+383] - \alpha_y^3(11+2\epsilon)[6(11+2\epsilon)\zeta_3+(22\epsilon+105)]+224\mathbf{r_f}\alpha_v^2\alpha_y+48\alpha_u\alpha_v\alpha_y(1+9\mathbf{r_f}), \tag{A44}$$

$$(\gamma_O^{(2)})_{31}\cdot\alpha_y^{-3/2} = -(11+2\epsilon)\mathbf{r_f}, \tag{A45}$$

$$(\gamma_O^{(3)})_{31}\cdot\alpha_y^{-3/2}=\frac{\alpha_g}{2}(11+2\epsilon)(1-\mathbf{r_c})\mathbf{r_f}+\frac{\alpha_u}{2}(11+2\epsilon)(5\mathbf{r_f}+9)\mathbf{r_f}+\alpha_v(11+2\epsilon)(6\mathbf{r_f}+1)\mathbf{r_f}+\alpha_y\mathbf{r_f}\left[2\mathbf{r_c}+\frac{473}{4}+38\epsilon+3\epsilon^2\right], \tag{A46}$$

$$(\gamma_O^{(1)})_{32}=12\mathbf{r_f}\alpha_u, \tag{A47}$$

$$(\gamma_O^{(2)})_{32}=2\alpha_y^2(11+2\epsilon)\mathbf{r_f}-112\alpha_u^2\mathbf{r_f}-24(1+9\mathbf{r_f})\alpha_u\alpha_v\mathbf{r_f}-24\alpha_u\alpha_y\mathbf{r_f}, \tag{A48}$$

$$\begin{aligned}(\gamma_O^{(3)})_{32}=&\alpha_g\alpha_u\alpha_y(1-\mathbf{r_c})\mathbf{r_f}[144\zeta_3-153]+\alpha_g\alpha_y^2(11+2\epsilon)(1-\mathbf{r_c})\mathbf{r_f}[28-36\zeta_3]+48\alpha_u\alpha_v\alpha_y[1+9\mathbf{r_f}]\mathbf{r_f}\\&+\alpha_u^2\alpha_v\mathbf{r_f}[4608\zeta_3\mathbf{r_f}+16(361\mathbf{r_f}-8)]+\alpha_u^3\mathbf{r_f}[384\zeta_3(1+4\mathbf{r_f})+4(437\mathbf{r_f}+141)]\\&+\alpha_u\alpha_v^2\mathbf{r_f}[576\zeta_3(1+7\mathbf{r_f})\mathbf{r_f}+12(\mathbf{r_f}(387\mathbf{r_f}+71)-4)]+\alpha_u\alpha_y^2\mathbf{r_f}\left[24(11+2\epsilon)\zeta_3+\frac{1}{2}(470\epsilon+2513)\right]\\&+\alpha_v\alpha_y^2(11+2\epsilon)\mathbf{r_f}[84\zeta_3\mathbf{r_f}+4(4+7\mathbf{r_f})]-\alpha_y^3\mathbf{r_f}(11+2\epsilon)[2(69+14\epsilon)+6(11+2\epsilon)\zeta_3]+224\alpha_u^2\alpha_y\mathbf{r_f},\end{aligned} \tag{A49}$$

$$(\gamma_O^{(1)})_{33}=3\alpha_y+8\alpha_u+4(1+4\mathbf{r_f})\alpha_v, \tag{A50}$$

$$(\gamma_O^{(2)})_{33}=-16\alpha_u\alpha_y+\frac{15\alpha_g\alpha_y}{2}(1-\mathbf{r_c})-248\mathbf{r_f}\alpha_u\alpha_v-2\alpha_v^2(85\mathbf{r_f}+37)\mathbf{r_f}-6\alpha_u^2(3+19\mathbf{r_f})-8\alpha_v\alpha_y(1+4\mathbf{r_f})-\frac{9\alpha_y^2}{4}(11+2\epsilon), \tag{A51}$$

$$\begin{aligned}(\gamma_O^{(3)})_{33}=&\alpha_g\alpha_u\alpha_y(1-\mathbf{r_c})(96\zeta_3-102)-\alpha_g^2\alpha_y(1-\mathbf{r_c})\left[27\zeta_3\mathbf{r_c}+\frac{3}{16}(-119\mathbf{r_c}+32\epsilon-13)\right]\\&+\alpha_g\alpha_v\alpha_y(1-\mathbf{r_c})(1+4\mathbf{r_f})[48\zeta_3-51]+\alpha_g\alpha_y^2(11+2\epsilon)(1-\mathbf{r_c})\left[\frac{303}{16}-33\zeta_3\right]\\&+\alpha_u^2\alpha_v[576\zeta_3(1+7\mathbf{r_f})\mathbf{r_f}+5562\mathbf{r_f}^2+3646\mathbf{r_f}+12]+\alpha_u^3[1152\zeta_3\mathbf{r_f}+4(602\mathbf{r_f}+59)]\\&+\alpha_u\alpha_v^2\mathbf{r_f}[4608\zeta_3\mathbf{r_f}+60(142\mathbf{r_f}+15)]+\alpha_u\alpha_y^2\left[12(11+2\epsilon)\zeta_3(2+9\mathbf{r_f})+23\epsilon\mathbf{r_f}+\frac{253\mathbf{r_f}}{2}+81\epsilon+\frac{843}{2}\right]\\&+\alpha_v^3\mathbf{r_f}[192\zeta_3(11\mathbf{r_f}+5)\mathbf{r_f}+2(\mathbf{r_f}(1484\mathbf{r_f}+927)+67)]+\frac{\alpha_v^2\alpha_y}{2}(659\mathbf{r_f}+275)\mathbf{r_f}\\&+\alpha_v\alpha_y^2\left[72(11+2\epsilon)\zeta_3\mathbf{r_f}+\epsilon(210\mathbf{r_f}+41)+1107\mathbf{r_f}+\frac{427}{2}\right]+454\mathbf{r_f}\alpha_u\alpha_v\alpha_y\\&-\alpha_y^3\left[\frac{9}{64}(11+2\epsilon)(82\epsilon+323)+(70-33\zeta_3)\mathbf{r_c}-70\mathbf{r_c}\right]+\frac{3}{2}\alpha_u^2\alpha_y(145\mathbf{r_f}+17)\end{aligned} \tag{A52}$$

$$(\gamma_O^{(1)})_{44}=\alpha_y, \tag{A53}$$

$$(\gamma_O^{(2)})_{44}=2\alpha_u^2(1+\mathbf{r_f})+2\alpha_v^2\mathbf{r_f}(1+\mathbf{r_f})+8\alpha_u\alpha_v\mathbf{r_f}-\frac{3}{4}(11+2\epsilon)\alpha_y^2+\frac{5}{2}\alpha_g\alpha_y(1-\mathbf{r_c}), \tag{A54}$$

$$(\gamma_O^{(3)})_{44} = \alpha_g^2\alpha_y(1-\mathbf{r_c})\left[\frac{1}{16}(119\mathbf{r_c}-32\epsilon+13)-9\zeta_3\mathbf{r_c}\right]-2\alpha_v^3(1+\mathbf{r_f})\mathbf{r_f}(1+4\mathbf{r_f})$$
$$+\alpha_g\alpha_y^2(11+2\epsilon)(1-\mathbf{r_c})\left[\frac{5}{16}-3\zeta_3\right]-\frac{15\alpha_v^2\alpha_y}{2}(1+\mathbf{r_f})\mathbf{r_f}+5\alpha_v\alpha_y^2(11+2\epsilon)\mathbf{r_f}$$
$$+\alpha_y^3\left[\frac{1}{64}(11+2\epsilon)(10\epsilon+183)+(3\zeta_3-2)\mathbf{r_c}\right]-30\alpha_u\alpha_v\alpha_y\mathbf{r_f}-4\alpha_u^3(1+4\mathbf{r_f})$$
$$+\frac{5\alpha_u\alpha_y^2}{2}(11+2\epsilon)(1+\mathbf{r_f})-12\alpha_u\alpha_v^2\mathbf{r_f}(1+4\mathbf{r_f})-6\alpha_u^2\alpha_v\mathbf{r_f}(3\mathbf{r_f}+7)-\frac{15\alpha_u^2\alpha_y}{2}(1+\mathbf{r_f}), \tag{A55}$$

$$(\gamma_O^{(1)})_{14}\cdot\alpha_y^{-1/2} = -4, \tag{A56}$$

$$(\gamma_O^{(2)})_{14}\cdot\alpha_y^{-1/2} = -10(1-\mathbf{r_c})\alpha_g+3(11+2\epsilon)\alpha_y, \tag{A57}$$

$$(\gamma_O^{(3)})_{14}\cdot\alpha_y^{-1/2} = -5\alpha_u\alpha_y(11+2\epsilon)(1+\mathbf{r_f})+\alpha_g^2(1-\mathbf{r_c})\left[36\zeta_3\mathbf{r_c}-\frac{1}{4}(119\mathbf{r_c}-32\epsilon+13)\right]-10\alpha_v\alpha_y(11+2\epsilon)\mathbf{r_f}$$
$$+\alpha_g\alpha_y(11+2\epsilon)(1-\mathbf{r_c})\left(12\zeta_3-\frac{5}{4}\right)-\alpha_y^2\left[\frac{1}{16}(11+2\epsilon)(10\epsilon+183)+(12\zeta_3+8)\mathbf{r_c}\right], \tag{A58}$$

$$(\gamma_O^{(2)})_{24} = -2\alpha_u(1+\mathbf{r_f})-4\alpha_v\mathbf{r_f}, \tag{A59}$$

$$(\gamma_O^{(3)})_{24} = \frac{15\alpha_u\alpha_y}{2}(1+\mathbf{r_f})+15\alpha_v\alpha_y\mathbf{r_f}+4\alpha_u^2(1+4\mathbf{r_f})$$
$$+4\alpha_u\alpha_v\mathbf{r_f}(3\mathbf{r_f}+7)+4\alpha_v^2\mathbf{r_f}(1+4\mathbf{r_f})-\frac{5\alpha_y^2}{4}(11+2\epsilon)(1+\mathbf{r_f}), \tag{A60}$$

$$(\gamma_O^{(2)})_{34} = -2\alpha_v(1+\mathbf{r_f})\mathbf{r_f}-4\alpha_u\mathbf{r_f}, \tag{A61}$$

$$(\gamma_O^{(3)})_{34} = 2\alpha_v^2(1+\mathbf{r_f})\mathbf{r_f}(1+4\mathbf{r_f})+\frac{15\alpha_v\alpha_y}{2}(1+\mathbf{r_f})\mathbf{r_f}-\frac{5\alpha_y^2}{2}(11+2\epsilon)\mathbf{r_f}$$
$$+15\alpha_u\alpha_y\mathbf{r_f}+2\alpha_u^2\mathbf{r_f}(3\mathbf{r_f}+7)+8\alpha_u\alpha_v\mathbf{r_f}(1+4\mathbf{r_f}). \tag{A62}$$

## APPENDIX B: OTHER APPROXIMATIONS FOR FINITE-$N_c$ FACTORS

In this appendix we provide the approximations for finite-$N_c$ factors obtained by fitting numerical data to the ratio of two second-order polynomials in $N_c$. The fixed-point factors are given as

$$f_g^{(1)} = \frac{N_c^2}{N_c^2-\frac{110}{19}}, \qquad f_g^{(2)} = \frac{N_c^2+6.750}{N_c^2-7.669}, \qquad f_g^{(3)} = \frac{N_c^2+26.937}{N_c^2-8.402},$$
$$f_y^{(1)} = \frac{N_c^2-1}{N_c^2-\frac{110}{19}}, \qquad f_y^{(2)} = \frac{N_c^2+5.578}{N_c^2-7.518}, \qquad f_y^{(3)} = \frac{N_c^2+23.618}{N_c^2-8.379},$$
$$f_u^{(1)} = \frac{N_c^2-0.9724}{N_c^2-\frac{110}{19}}, \qquad f_u^{(2)} = \frac{N_c^2+5.612}{N_c^2-7.545}, \qquad f_u^{(3)} = \frac{N_c^2+25.240}{N_c^2-8.395},$$
$$f_v^{(1)} = \frac{N_c^2-0.9393}{N_c^2-\frac{110}{19}}, \qquad f_v^{(2)} = \frac{N_c^2+4.233}{N_c^2-7.355}, \qquad f_v^{(3)} = \frac{N_c^2+17.972}{N_c^2-8.278}. \tag{B1}$$

The factors for the field anomalous dimensions and that of $m_\phi^2$ are

$$
\begin{aligned}
f_H^{(1)} &= \frac{N_c^2-1}{N_c^2-\frac{110}{19}}, & f_H^{(2)} &= \frac{N_c^2+5.855}{N_c^2-7.543}, & f_H^{(3)} &= \frac{N_c^2+27.656}{N_c^2-8.415},\\
f_\psi^{(1)} &= \frac{N_c^2-1}{N_c^2-\frac{110}{19}}, & f_\psi^{(2)} &= \frac{N_c^2+8.285}{N_c^2-7.747}, & f_\psi^{(3)} &= \frac{N_c^2+31.882}{N_c^2-8.448},\\
f_{m^2}^{(1)} &= \frac{N_c^2-0.999}{N_c^2-\frac{110}{19}}, & f_{m^2}^{(2)} &= \frac{N_c^2+21.855}{N_c^2-7.977}, & f_{m^2}^{(3)} &= \frac{N_c^2+114.062}{N_c^2-8.562},\\
f_{G(c)}^{(1)} &= \frac{N_c^2}{N_c^2-\frac{110}{19}}, & f_{G(c)}^{(2)} &= \frac{N_c^2+6.959}{N_c^2-7.707}, & f_{G(c)}^{(3)} &= \frac{N_c^2+29.766}{N_c^2-8.437}.
\end{aligned}
\tag{B2}
$$

The critical exponents corresponding to dimension-four operators are corrected by

$$
\begin{aligned}
f_{\theta_1}^{(2)} &= \frac{N_c^2}{N_c^2-\frac{110}{19}}, & f_{\theta_1}^{(3)} &= \frac{N_c^2+4.15}{N_c^2-7.085}, & f_{\theta_1}^{(4)} &= \frac{N_c^2+30.8}{N_c^2-8.403},\\
f_{\theta_2}^{(1)} &= \frac{N_c^2-1}{N_c^2-\frac{110}{19}}, & f_{\theta_2}^{(2)} &= \frac{N_c^2+5.71}{N_c^2-7.507}, & f_{\theta_2}^{(3)} &= \frac{N_c^2+29.7}{N_c^2-8.473},\\
f_{\theta_3}^{(1)} &= \frac{N_c^2-0.9103}{N_c^2-5.78323}, & f_{\theta_3}^{(2)} &= \frac{N_c^2+5.01}{N_c^2-7.5524}, & f_{\theta_3}^{(3)} &= \frac{N_c^2+32.9}{N_c^2-8.4346},\\
f_{\theta_4}^{(1)} &= \frac{N_c^2-1.175}{N_c^2-5.8011}, & f_{\theta_4}^{(2)} &= \frac{N_c^2+29.5}{N_c^2-7.891}, & f_{\theta_4}^{(3)} &= \frac{N_c^2+144}{N_c^2-8.543}.
\end{aligned}
\tag{B3}
$$

The approximate expressions for the two nontrivial eigenvalues for $\gamma_O^*$ are given as

$$
\begin{aligned}
f_{\gamma_3}^{(1)} &= \frac{N_c^2-1.153}{N_c^2-5.7996}, & f_{\gamma_3}^{(2)} &= \frac{N_c^2+15.14}{N_c^2-7.856}, & f_{\gamma_3}^{(3)} &= \frac{N_c^2+71.03}{N_c^2-8.5345},\\
f_{\gamma_4}^{(1)} &= \frac{N_c^2-0.919}{N_c^2-5.7839}, & f_{\gamma_4}^{(2)} &= \frac{N_c^2+6.04}{N_c^2-7.6215}, & f_{\gamma_4}^{(3)} &= \frac{N_c^2+32}{N_c^2-8.4419}.
\end{aligned}
\tag{B4}
$$


[1] David J. Gross and Frank Wilczek, Ultraviolet behavior of non-Abelian gauge theories, Phys. Rev. Lett. **30**, 1343 (1973).

[2] H. David Politzer, Reliable perturbative results for strong interactions?, Phys. Rev. Lett. **30**, 1346 (1973).

[3] Steven Weinberg, Ultraviolet divergences in quantum theories of gravitation, in *General Relativity: An Einstein Centenary Survey* (Oxford University Press, Cambridge, 1979), pp. 790–831.

[4] Claudio Pica and Francesco Sannino, UV and IR zeros of gauge theories at the four loop order and beyond, Phys. Rev. D **83**, 035013 (2011).

[5] Daniel F. Litim and Francesco Sannino, Asymptotic safety guaranteed, J. High Energy Phys. 12 (2014) 178.

[6] Andrew D. Bond and Daniel F. Litim, More asymptotic safety guaranteed, Phys. Rev. D **97**, 085008 (2018).

[7] Borut Bajc and Francesco Sannino, Asymptotically safe grand unification, J. High Energy Phys. 12 (2016) 141.

[8] Andrew D. Bond and Daniel F. Litim, Asymptotic safety guaranteed in supersymmetry, Phys. Rev. Lett. **119**, 211601 (2017).

[9] Borut Bajc, Manuel Del Piano, and Francesco Sannino, UV finite GUT with SUSY breaking, arXiv:2308.13311.

[10] Astrid Eichhorn and Marc Schiffer, Asymptotic safety of gravity with matter, arXiv:2212.07456.

[11] Alexander Bednyakov and Alfiia Mukhaeva, Perturbative asymptotic safety and its phenomenological applications, Symmetry **15**, 1497 (2023).

[12] Oleg Antipin, Marc Gillioz, Esben Mølgaard, and Francesco Sannino, The $a$ theorem for gauge-Yukawa theories beyond Banks-Zaks fixed point, Phys. Rev. D **87**, 125017 (2013).

[13] Andrew D. Bond, Daniel F. Litim, Gustavo Medina Vazquez, and Tom Steudtner, UV conformal window for asymptotic safety, Phys. Rev. D **97**, 036019 (2018).

[14] Andrew D. Bond, Daniel F. Litim, and Gustavo Medina Vazquez, Conformal windows beyond asymptotic freedom, Phys. Rev. D **104**, 105002 (2021).
[15] Daniel F. Litim, Matin Mojaza, and Francesco Sannino, Vacuum stability of asymptotically safe gauge-Yukawa theories, J. High Energy Phys. 01 (2016) 081.
[16] Francesco Sannino and Ian M. Shoemaker, Asymptotically safe dark matter, Phys. Rev. D **92**, 043518 (2015).
[17] Niklas Grønlund Nielsen, Francesco Sannino, and Ole Svendsen, Inflation from asymptotically safe theories, Phys. Rev. D **91**, 103521 (2015).
[18] Dirk H. Rischke and Francesco Sannino, Thermodynamics of asymptotically safe theories, Phys. Rev. D **92**, 065014 (2015).
[19] Alessandro Codello, Kasper Langæble, Daniel F. Litim, and Francesco Sannino, Conformal gauge-Yukawa theories away from four dimensions, J. High Energy Phys. 07 (2016) 118.
[20] Andrew D. Bond, Gudrun Hiller, Kamila Kowalska, and Daniel F. Litim, Directions for model building from asymptotic safety, J. High Energy Phys. 08 (2017) 004.
[21] Nicola Andrea Dondi, Vladimir Prochazka, and Francesco Sannino, Conformal data of fundamental gauge-Yukawa theories, Phys. Rev. D **98**, 045002 (2018).
[22] Kamila Kowalska, Andrew Bond, Gudrun Hiller, and Daniel Litim, Towards an asymptotically safe completion of the standard model, Proc. Sci. EPS-HEP2017 (**2017**) 542.
[23] Steven Abel and Francesco Sannino, Radiative symmetry breaking from interacting UV fixed points, Phys. Rev. D **96**, 056028 (2017).
[24] Nicolai Christiansen, Astrid Eichhorn, and Aaron Held, Is scale-invariance in gauge-Yukawa systems compatible with the graviton?, Phys. Rev. D **96**, 084021 (2017).
[25] Francesco Sannino and Vedran Skrinjar, Instantons in asymptotically safe and free quantum field theories, Phys. Rev. D **99**, 085010 (2019).
[26] Daniele Barducci, Marco Fabbrichesi, Carlos M. Nieto, Roberto Percacci, and Vedran Skrinjar, In search of a UV completion of the standard model—378,000 models that don't work, J. High Energy Phys. 11 (2018) 057.
[27] Gudrun Hiller, Clara Hormigos-Feliu, Daniel F. Litim, and Tom Steudtner, Anomalous magnetic moments from asymptotic safety, Phys. Rev. D **102**, 071901 (2020).
[28] Gudrun Hiller, Clara Hormigos-Feliu, Daniel F. Litim, and Tom Steudtner, Asymptotically safe extensions of the standard model with flavour phenomenology, in *Proceedings of the 54th Rencontres de Moriond on Electroweak Interactions and Unified Theories* (ARISF, 2019), pp. 415–418, arXiv:1905.11020.
[29] Gudrun Hiller, Clara Hormigos-Feliu, Daniel F. Litim, and Tom Steudtner, Model building from asymptotic safety with Higgs and flavor portals, Phys. Rev. D **102**, 095023 (2020).
[30] Stefan Bißmann, Gudrun Hiller, Clara Hormigos-Feliu, and Daniel F. Litim, Multi-lepton signatures of vector-like leptons with flavor, Eur. Phys. J. C **81**, 101 (2021).
[31] Rigo Bause, Gudrun Hiller, Tim Höhne, Daniel F. Litim, and Tom Steudtner, B-anomalies from flavorful U(1)′ extensions, safely, Eur. Phys. J. C **82**, 42 (2022).
[32] Gudrun Hiller, Daniel F. Litim, and Kevin Moch, Fixed points in supersymmetric extensions of the standard model, Eur. Phys. J. C **82**, 952 (2022).
[33] Gudrun Hiller, Tim Höhne, Daniel F. Litim, and Tom Steudtner, Portals into Higgs vacuum stability, Phys. Rev. D **106**, 115004 (2022).
[34] Domenico Orlando, Susanne Reffert, and Francesco Sannino, A safe CFT at large charge, J. High Energy Phys. 08 (2019) 164.
[35] Oleg Antipin, Jahmall Bersini, and Pantelis Panopoulos, Yukawa interactions at large charge, J. High Energy Phys. 10 (2022) 183.
[36] Soo-Jong Rey and Francesco Sannino, Safe gauge-string correspondence, Nucl. Phys. **B985**, 116003 (2022).
[37] Daniel F. Litim, Nahzaan Riyaz, Emmanuel Stamou, and Tom Steudtner, Asymptotic safety guaranteed at four loop, Phys. Rev. D **108**, 076006 (2023).
[38] Gerard 't Hooft, A planar diagram theory for strong interactions, Nucl. Phys. **B72**, 461 (1974).
[39] G. Veneziano, Some aspects of a unified approach to gauge, dual and Gribov theories, Nucl. Phys. **B117**, 519 (1976).
[40] A. Bednyakov and A. Pikelner, Six-loop beta functions in general scalar theory, J. High Energy Phys. 04 (2021) 233.
[41] M. Tentyukov and J. Fleischer, A Feynman diagram analyzer DIANA, Comput. Phys. Commun. **132**, 124 (2000).
[42] Paulo Nogueira, Automatic Feynman graph generation, J. Comput. Phys. **105**, 279 (1993).
[43] J. Kuipers, T. Ueda, J. A. M. Vermaseren, and J. Vollinga, FORM version 4.0, Comput. Phys. Commun. **184**, 1453 (2013).
[44] Matthias Steinhauser, MATAD: A program package for the computation of MAssive TADpoles, Comput. Phys. Commun. **134**, 335 (2001).
[45] A. A. Vladimirov, Method for computing renormalization group functions in dimensional renormalization scheme, Theor. Math. Phys. **43**, 417 (1980).
[46] Mikolaj Misiak and Manfred Munz, Two loop mixing of dimension five flavor changing operators, Phys. Lett. B **344**, 308 (1995).
[47] F. Jegerlehner, Facts of life with $\gamma_5$, Eur. Phys. J. C **18**, 673 (2001).
[48] K. G. Chetyrkin and M. F. Zoller, Three-loop $\beta$-functions for top-Yukawa and the Higgs self-interaction in the standard model, J. High Energy Phys. 06 (2012) 033.
[49] A. V. Bednyakov, A. F. Pikelner, and V. N. Velizhanin, Higgs self-coupling beta-function in the standard model at three loops, Nucl. Phys. **B875**, 552 (2013).
[50] I. Jack and H. Osborn, Constraints on RG flow for four dimensional quantum field theories, Nucl. Phys. **B883**, 425 (2014).
[51] Oleg Antipin, Marc Gillioz, Jens Krog, Esben Mølgaard, and Francesco Sannino, Standard model vacuum stability and Weyl consistency conditions, J. High Energy Phys. 08 (2013) 034.
[52] C. Poole and A. E. Thomsen, Weyl consistency conditions and $\gamma_5$, Phys. Rev. Lett. **123**, 041602 (2019).
[53] Colin Poole and Anders Eller Thomsen, Constraints on 3- and 4-loop $\beta$-functions in a general four-dimensional quantum field theory, J. High Energy Phys. 09 (2019) 055.

[54] Anders Eller Thomsen, Introducing RGBeta: A *Mathematica* package for the evaluation of renormalization group $\beta$-functions, Eur. Phys. J. C **81**, 408 (2021).

[55] Alexander Bednyakov and Andrey Pikelner, Four-loop gauge and three-loop Yukawa beta functions in a general renormalizable theory, Phys. Rev. Lett. **127**, 041801 (2021).

[56] Joshua Davies, Florian Herren, and Anders Eller Thomsen, General gauge-Yukawa-quartic $\beta$-functions at 4-3-2-loop order, J. High Energy Phys. 01 (2022) 051.

[57] Daniel F. Litim and Tom Steudtner, ARGES—Advanced renormalisation group equation simplifier, Comput. Phys. Commun. **265**, 108021 (2021).

[58] Ingo Schienbein, Florian Staub, Tom Steudtner, and Kseniia Svirina, Revisiting RGEs for general gauge theories, Nucl. Phys. **B939**, 1 (2019); **B966**, 115339(E) (2021).

[59] See Supplemental Material at http://link.aps.org/supplemental/10.1103/PhysRevD.109.065030 for the analytical expressions of the RG functions, the values of the couplings and anomalous dimensions at the fixed point, and our numerical fit to finite $N_c$ corrections.

[60] Steven Weinberg, Phenomenological Lagrangians, Physica (Amsterdam) **A96**, 327 (1979).

[61] A. J. Paterson, Coleman-Weinberg symmetry breaking in the chiral $\mathrm{SU}(N) \times \mathrm{SU}(N)$ linear sigma model, Nucl. Phys. **B190**, 188 (1981).